Design and Construction of LG-3 Powerhouse Roof

Sami Bebawi

A Major Technical Report

in

The Department

of

Civil Engineering

Presented in Partial Fulfilment of the Requirements
for the degree of Master of Engineering at
Concordia University
Montréal, Québec, Canada

April 1984

ABSTRACT

DESIGN AND CONSTRUCTION OF LG-3 POWERHOUSE ROOF

Sami Bébawi

The principal objective of this report is to present the methods and techniques employed in the design and construction of a powerhouse roof. The evolution of this design is discussed in the second chapter of this report. The design details of the top wearing slab are developed using manual and computer computations. The design of other elements, such as the deck plates and the open type rib beams was presented only in general terms. The deck plate and the structural slab were connected by shear studs, thus, a composite orthotropic action was obtained. This design eliminated the need for a shoring system during construction. In the third chapter, more emphasis was given to the technical specifications and the quality control measures which were necessary to verify the considerable amount of welds. Also explained are the problems encountered in the field during construction.

DESIGN ET CONSTRUCTION DE LA TOITURE DE LA CENTRALE DE LG-3

RESUME

L'objectif principal de ce rapport est de présenter les méthodes et techniques employées dans le design et la construction d'une toiture de centrale. Les différents stages d'évolution du design sont discutés dans le second chapitre du rapport et les détails du design de la dalle de surface sont développés en utilisant les calculs manuels et d'ordinateur. Le design des autres éléments, tels la plaque de pontage et les raidisseurs est présenté seulement en termes généraux. La plaque de pontage et la dalle structurale sont connectées par des goujons de cisaillement, ce qui permet donc d'obtenir une action orthotropique. Ce design a éliminé la nécessité de systèmes d'étaiement durant la construction. Au troisième chapitre, plus d'emphase est accordée aux spécifications techniques et aux mesures de contrôle de la qualité qui se sont avérés nécessaires pour vérifier la quantité considérable de soudure. Sont également expliqués les problèmes rencontrés au chantier durant la construction.

To my Beloved wife and children

for the time I have taken away

from them to complete this degree

ACKNOWLEDGEMENTS

The work presented in this report is a result of the efforts of many sincere individuals who worked together, either in the design and construction stages. I had the pleasure of being part of the design team of SNC-Cartier and of the construction group in S.E.B.J's, administrative field office. During the early stages of design, I had the opportunity to discuss the soundness of our approach to this new type of roof structure with Professor M.S. Troitsky, and his advice and constructive criticism were invaluable.

The writer is indebted to the interest and helpful suggestions of Mr. P. Jeanty. Thanks are also due to Mr. B. Mc-Iver for his precise reviewing of this report. I am equally grateful to Mrs I. Jeanty for her patience and excellent typing of this manuscript.

TABLE OF CONTENTS

LIST OF FIGURES

LIST OF TABLES

LIST OF PHOTOS

CHAPTER 1

THE JAMES BAY HYDROELECTRIC COMPLEX

Introduction

In 1971 the Government of Quebec created a public corporation named La Société d'Energie de la Baie James (SEBJ) to manage the engineering and construction of the "La Grande Complex". SEBJ is a wholy owned subsidiary of Hydro-Quebec.

The First phase of "The Complex" includes the construction of three powerhouses on the La Grande Rivière and the diversion of water from the watersheds of the Eastmain and Caniapiscau rivers. "The Complex" is being constructed in an area of only slight topographical relief located in northern Quebec. Thus, major reservoirs are required, necessitating the construction of a total of 182 dykes requiring some 150 milion cubic metres of fill.

The LG-2 powerhouse, the only one which is underground, will provide more than half of the 10,269 megawatts that "The Complex" will inject into Hydro-Quebec's network. The commissioning of the generating units began in 1979 and will continue through 1985. Plans originally called for the construction of a fourth powerhouse, LG-1 but when "The Complex" was divided into two phases, the construction of LG-1 was included in the second phase.

La Grande Complex - Phase 1

Power-house	Number of Units	Unit Capacity (MW)	Installed Capacity (MW)	Guaranted Annual Output (TWh)	Commissioning of First Unit
LG-2	16	333	5328	35.8	October 79
LG-3	12	192	2304	12.3	July 82
LG-4	9	293	2637	14.1	Feb. 84
Total	37	-	10269	62.2	

LG-3 is a surface powerhouse. In order to prepare for the construction of the powerhouse a total of 317,000 cubic yards of bedrock had to be excavated. This is in addition to the underground excavation of the twelve penstocks (one for each of the twelve generating units). A total of 190,000 cubic yards of concrete were used in the construction of the powerhouse, 130,000 cubic yards for the spillway and 136,600 cu. yards for the intake structure.

1.1 LG-3, Powerhouse: Layout

The general arrangement of the powerhouse is affected to a considerable degree by its location with respect to the intake structure (Fig. 1.1). As usual, the distance between the two structures was first established on the basis of an economic evaluation, taking into account the cost of the penstocks and of the open-cut excavation for the powerhouse and tailrace channel. Since the rock from the powerhouse and tailrace excavation was used for the construction of the main dam, the economic comparison of alternative locations for the powerhouse resulted in a relatively short distance between the intake and the powerhouse. Due to the fact that the dam bridges the penstocks, it was necessary to introduce a second criterion, namely that a line extending from the toe of the dam at an angle of 45° would not intersect any excavation for the powerhouse. It is perhaps of interest to note that without this second criterion the powerhouse would be located even closer to the intake thereby reducing the high cost of steel lined penstocks.

In the layout of the powerhouse every effort was made to reduce the enclosed space to a minimum. This would not only reduce the initial construction costs but also minimize the cost of heating and maintenance (Fig. 1.2 & 1.3). It was also very important to reduce the distance between the scroll cases to a minimum, since any reduction in this dimension is multiplied by eleven (Fig. 1.4 & 1.5). Construction of the units commences from the service bay so that, aside from other considerations, the crane columns will be adequately supported

in the lateral direction to permit lifting of the heaviest loads. It was assumed that during the concreting of the first steel scroll case, the welding of the adjacent one would still be in progress. It was consequently assumed that a free space of 5 feet between the form-work and the adjacent scroll case would provide sufficient access for the turbine installer. A minimum of three feet was adopted for the concrete encasement of the scroll case. The total distance between the outside shells of two adjacent scroll cases is therefore eight feet, with a contraction joint in the concrete between each unit. The resulting centre-to-centre distance between each unit is 71 feet. Other proposed criteria regarding a minimum distance between penstock tunnels and the placement of mechanical equipment were subsequently met. For example, it is always possible to control blasting during the excavation phase of the penstocks so that the remaining rock between the penstock cavities is left undisturbed. Eventually the penstocks are lined with concrete and the surrounding rock grouted, thus re-establishing to a large extent, the structural integrity of the rock formation.

An additional economy in minimizing the length of the powerhouse could have been obtained by minimizing the length of the unloading and service bay. Although three rotors may be in this area at one time during the construction stage, this does not justify the provision of space for more than two units on a permanent basis. To provide the required floor area for a third rotor during construction, a careful and detailed study was performed and the area later occupied by offices, storerooms etc. was utilised as additional work space.

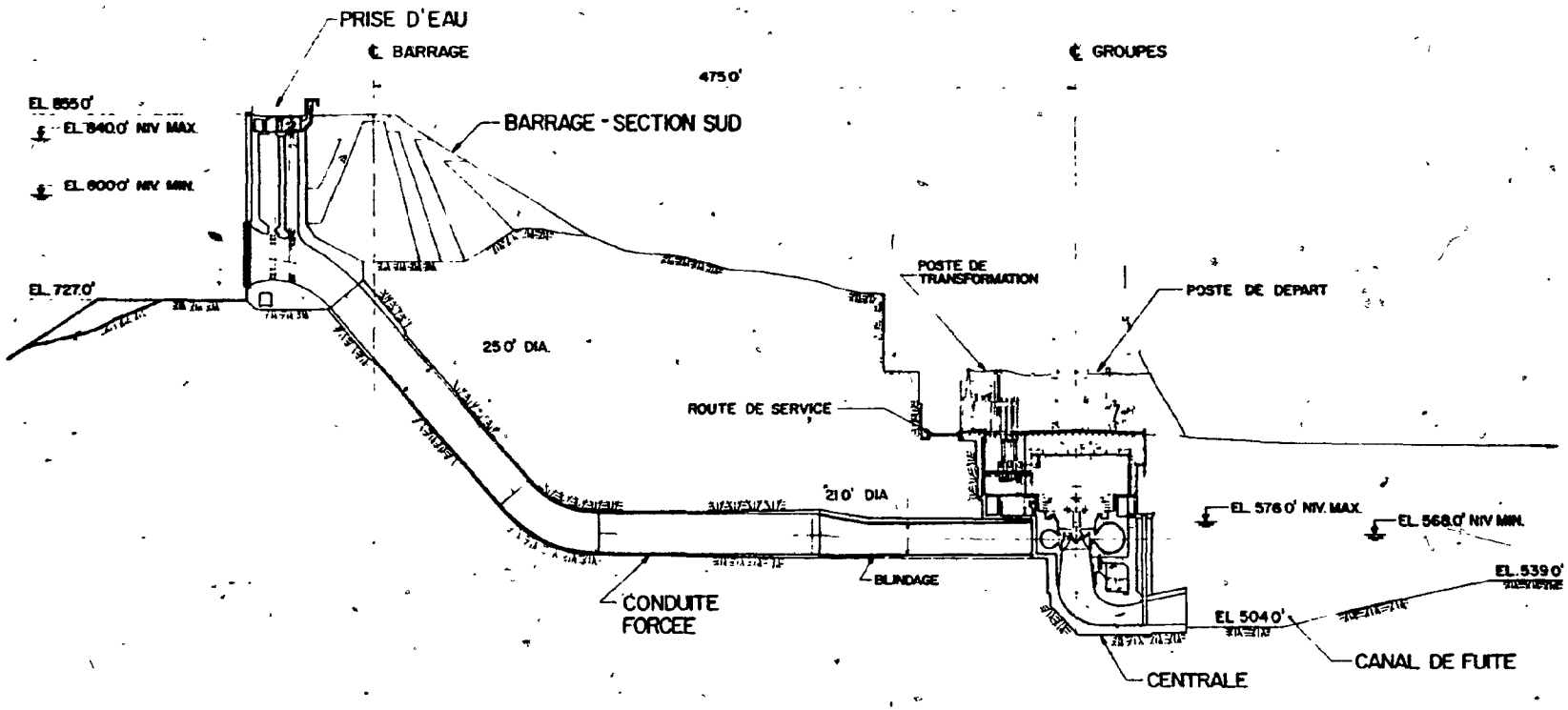

Fig. 1.1 Typical Lay-Out of LG-3 main dam and powerhouse.

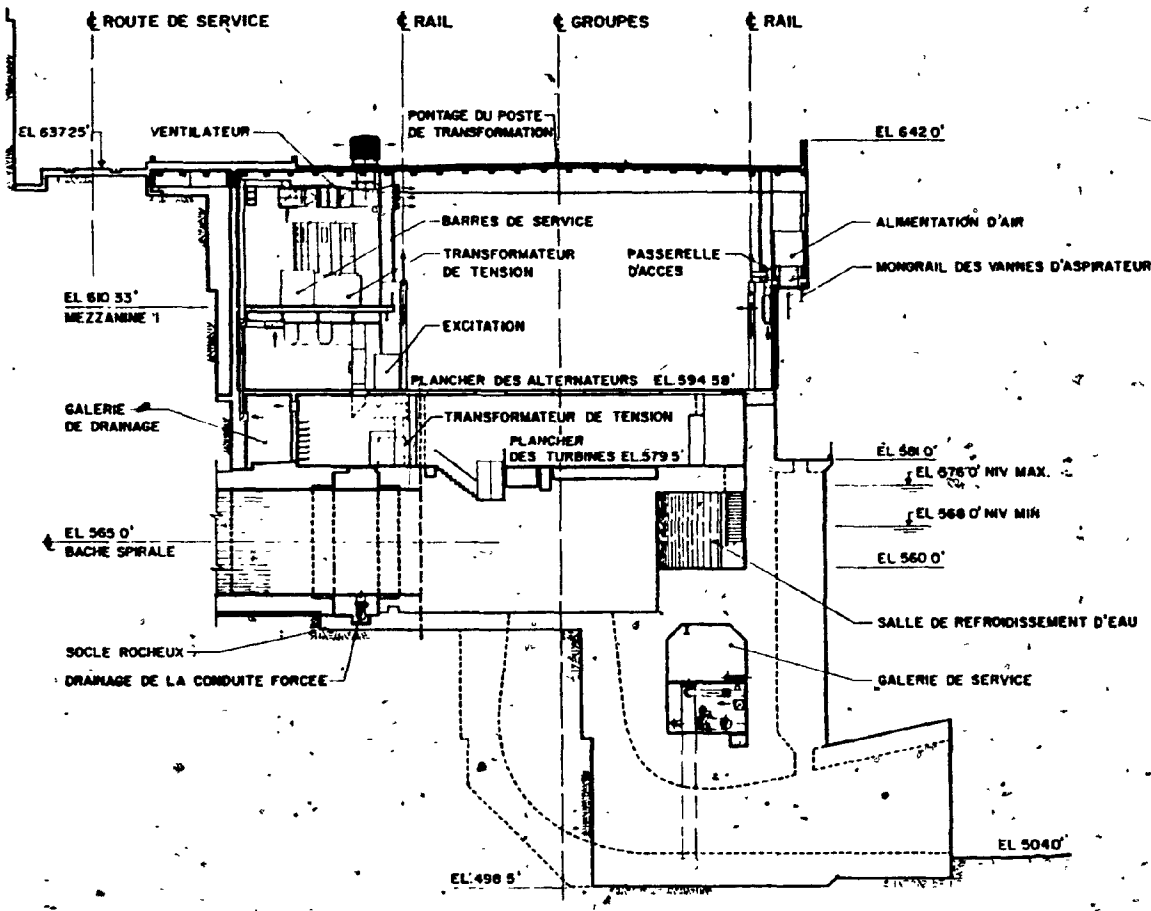

Fig. 1.2 LG-3 Powerhouse, Cross-Section.

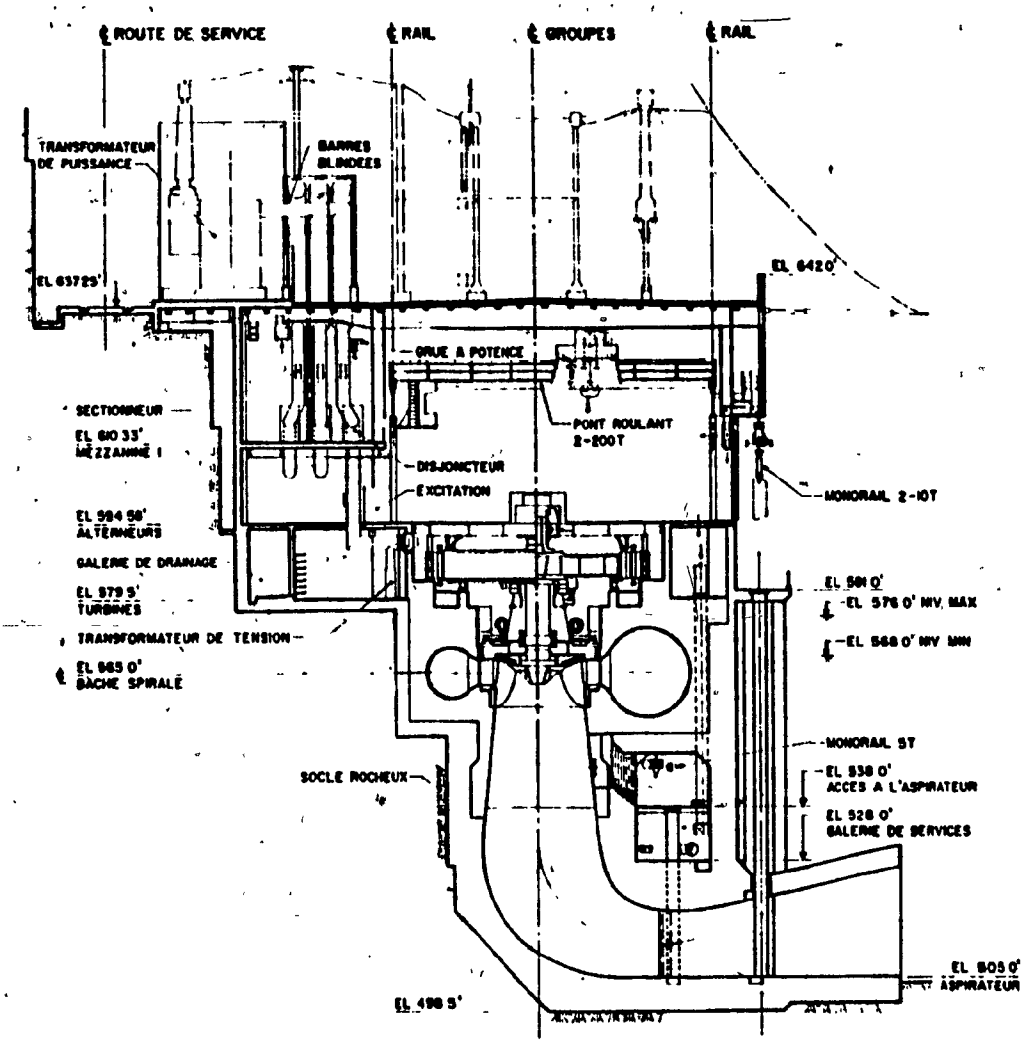

Fig. 1.3 LG-3 Powerhouse, Cross-Section.

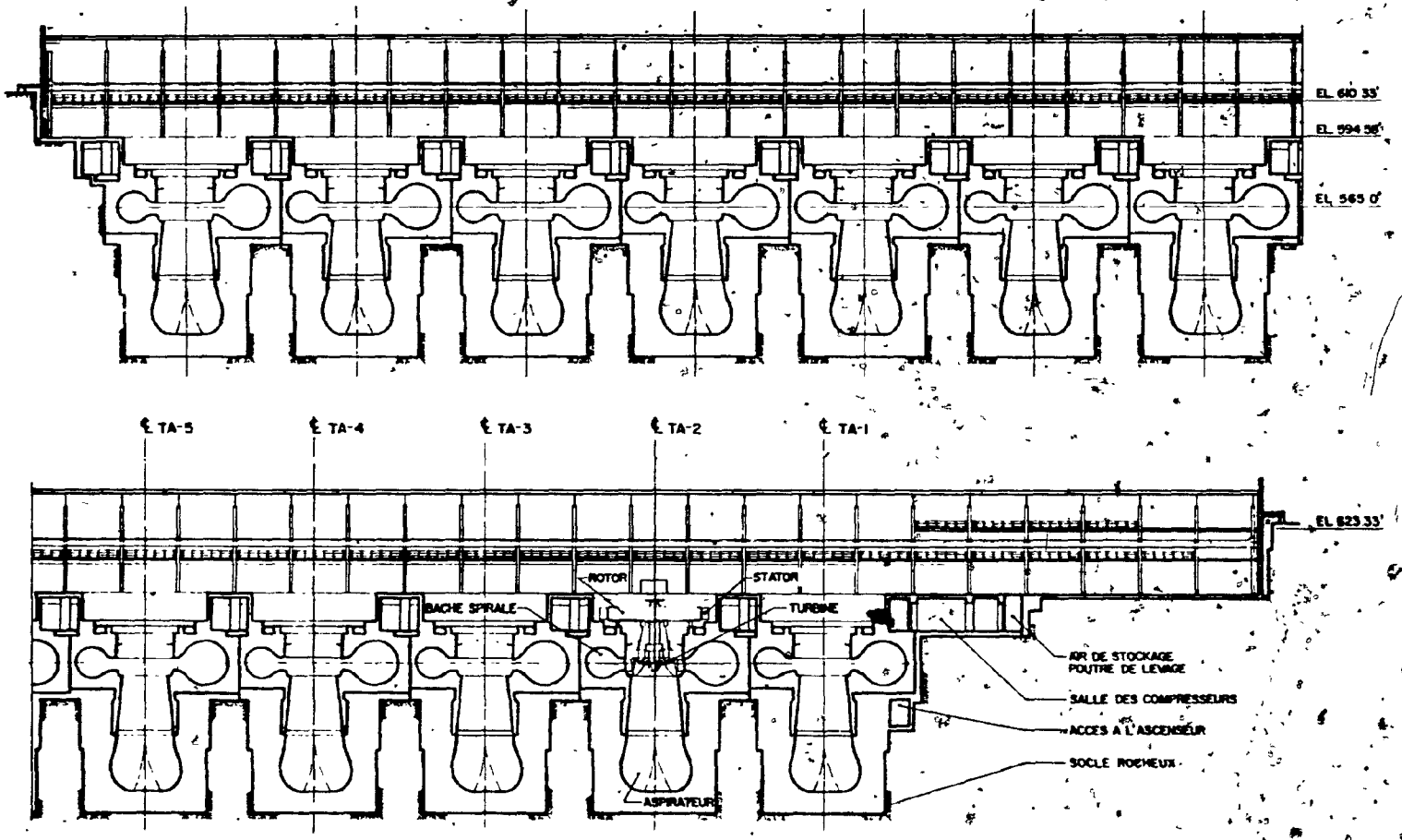

Fig. 1.4 LG-3 Powerhouse Longitudinal Section.

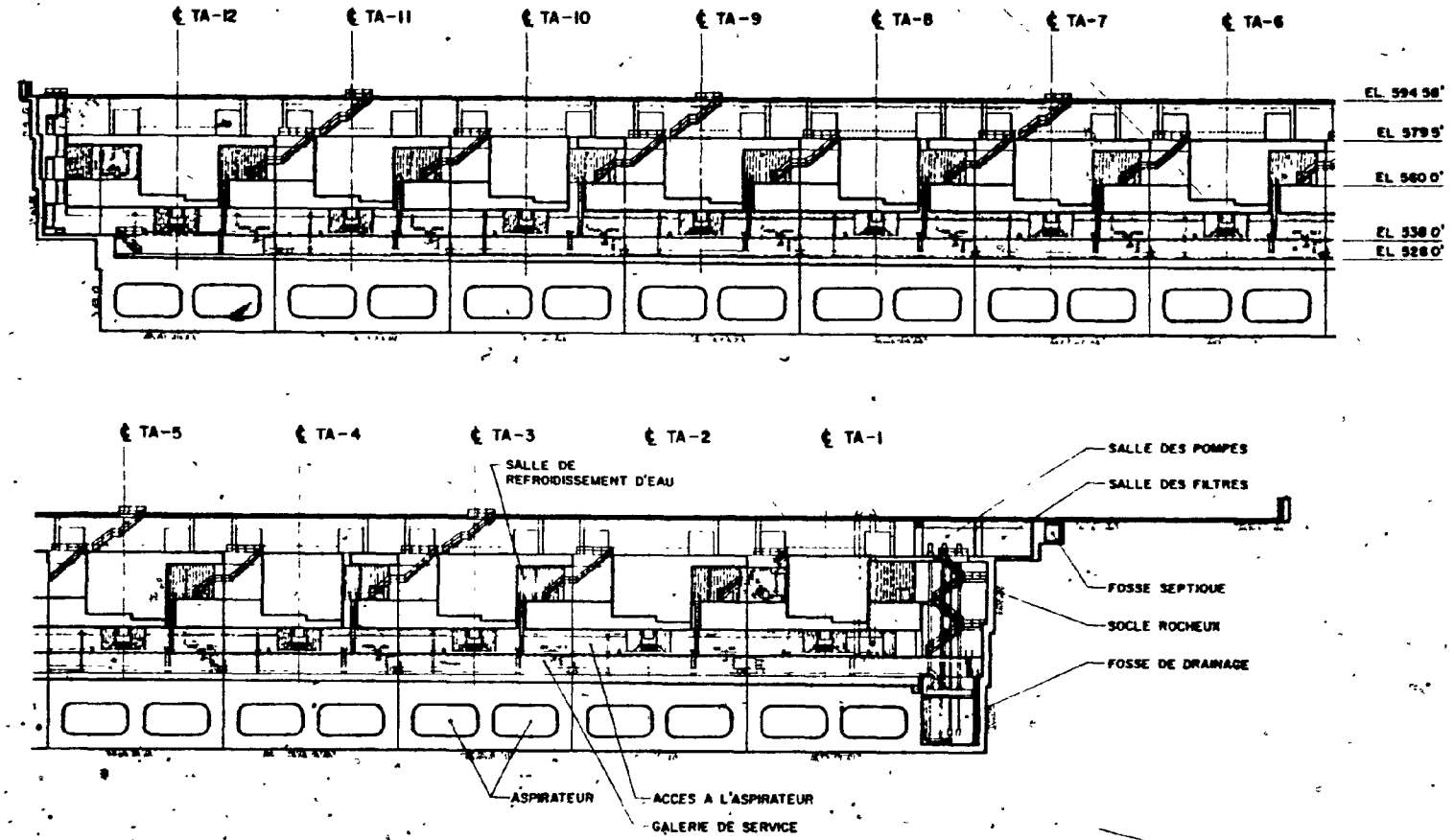

Fig. 1.5 LG-3 Powerhouse Longitudinal Section.

The width and height of the machine hall are a function of the size of the equipment. Obviously the minimization of the distance between the upstream and downstream columns automatically minimizes the cost and dead weight of the bridge cranes and roof beams. The height beneath the crane hook was determined by the requirement that the generator rotor and all other dismantled components of the turbine or generator, must safely pass over operating units. At the turbine level, the powerhouse extends upstream from the machine hall to accomodate the cable gallery and the drainage gallery; the latter having a width of eight feet to accomodate drilling equipment to enable grouting of the upstream wall. The primary excavation was tailored to suit the minimum dimensions of the powerhouse. It must be admitted though that the original approach was not very succesful in maintaining the excavation within the limits shown on the drawings; this is particularly true for the step between the turbine and generator level.

In fact it became necessary to revise the concrete drawings to suit the actual excavation, thus reducing the quantity of backfill concrete required by relocating the upstream structural wall. In this case, the primary excavation and subsequent placement of concrete was carried out by two different contractors. Future problems in a similar situation could be avoided by introducing penalties for over-excavation.

The generator floor level is determined by the position of the turbines and the dimensions of the turbine-generator unit. In the case of LG-3 this brings the generator floor well above the maximum tailwater level. Therefore, the drainage water collected upstream of

the powerhouse can be diverted by gravity to the tailwater level. The concrete at the generator floor level extends to the upstream rock face, thus sealing the drainage gallery beneath against surface run-off and accidental direct communication with the tailwater. The upstream wall of the drainage gallery is completely concrete lined with holes drilled through the lining into the rock to the end of the steel liner of the penstocks. These holes serve to drain the water seepage in the rock mass which is largely caused by the elevated pressure in the concrete lined sections of the penstocks.

In response to Hydro-Quebec's recommandation, the switchyard was placed on the roof of the powerhouse (Fig. 1.3).

Access to the switchyard is provided by a road excavated in the rock to the roof level. In addition, this rock berm serves as an anchor for the horizontal forces imposed on the roof structure by the transmission lines.

CHAPTER 2

EVOLUTION OF THE SUPERSTRUCTURE DESIGN

A survey of the roofs of other Hydro-Quebec installations established that there were problemes with conventional roofs on most of the powerhouse, and that their maintenance was difficult and costly. The placement of various equipment on top of the numerous foundation blocks, combined with the problem caused by the traffic during erection or repair increased the risk of water leakage from the roof. Taking the aforementioned factors into consideration and also on view of very severe climatic conditions in the LG-3 region (the temperature can vary between +30°C in summer and -40°C in winter), the choice of the roof system was made after a detailed study of several alternatives; the most important ones being the following:

2.1 Alternative no. 1

As a first approach, a conventional roof system consisting of beams spaced 10 feet centre-to-centre spanning between either rigid frames or a truss-type structure supporting a corrugated metal deck with a six inch concrete slab was choosen (Fig. 2.1). Water tightness was to be assured by an inverse membrane system consisting of a membrane, a layer of rigid thermal insulation and then four inches of concrete protection (a wearing slab) to permit heavy traffic on the whole surface. The choice between a rigid frame or an open truss-type structure

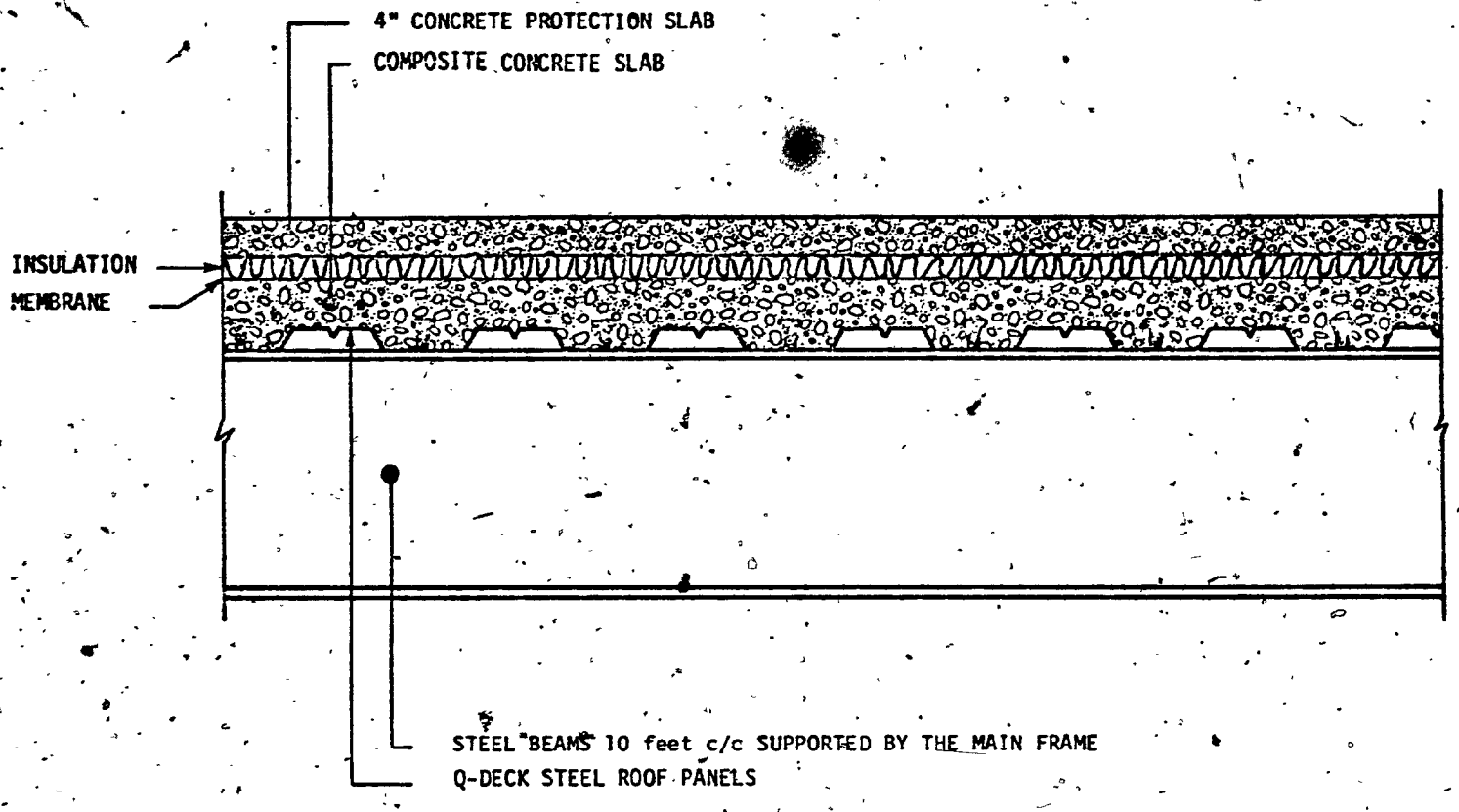

Fig. 2.1 ALTERNATIVE Nº I

was subjected to many discussions and economic analyses (Fig. 2.2 and 2.3). On one hand the truss was found to be lighter than a rigid frame, but it would take more time to erect. Mechanical ducts and pipes could easily be placed through the truss members using standard supporting elements, whereas with a rigid frame, web openings should be provided if the top elevation of the roof was to be kept unchanged. Such openings in the rigid frame's web would have to be carefully checked so that stress concentrations would not exceed the allowable design loads. In general, the truss proved to be less expensive but the stiffness and the appearance of a rigid frame succeeded in overriding the economic advantage of the truss.

A concrete wearing slab resting on top of thermal insulation panels while subjected to the heavy traffic loads proved to be very complicated. A minimum thickness had to be determined using a rather detailed design, since any economy in the overall thickness of this protection slab would have a pronounced effect on the total dead loads applied to the roof main supporting elements. The following study shows the detailed analysis which was necessary to determine the properties of the roof slab.

2.1.1 Design Criteria

Due to considerable traffic on the roof caused by the circulation of a mobile crane, a wearing slab was necessary to improve traction and to protect the insulation material.

The principal requirements of this wearing slab may be

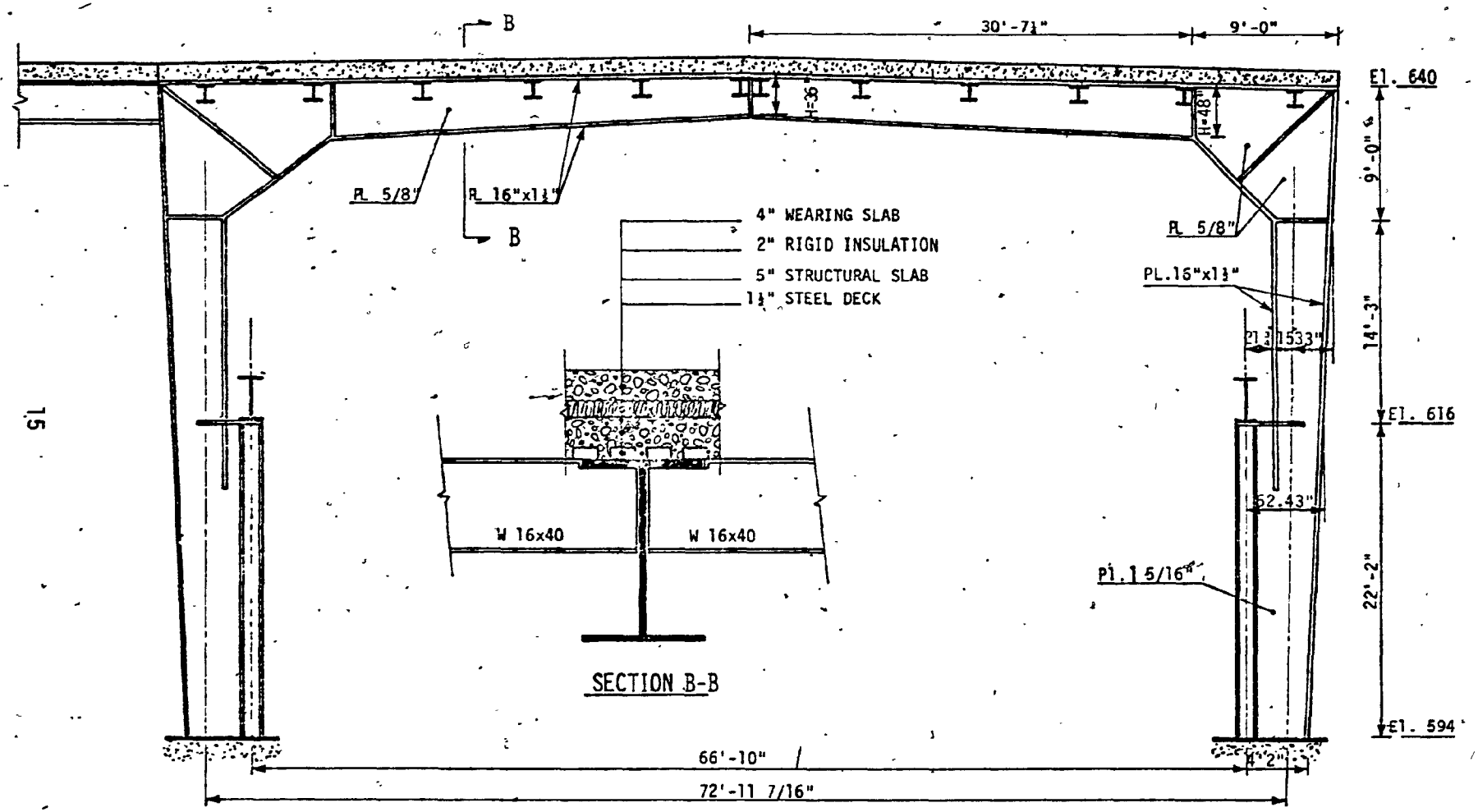

Fig. 2.2 Proposed rigid frame for LG-3 Powerhouse.

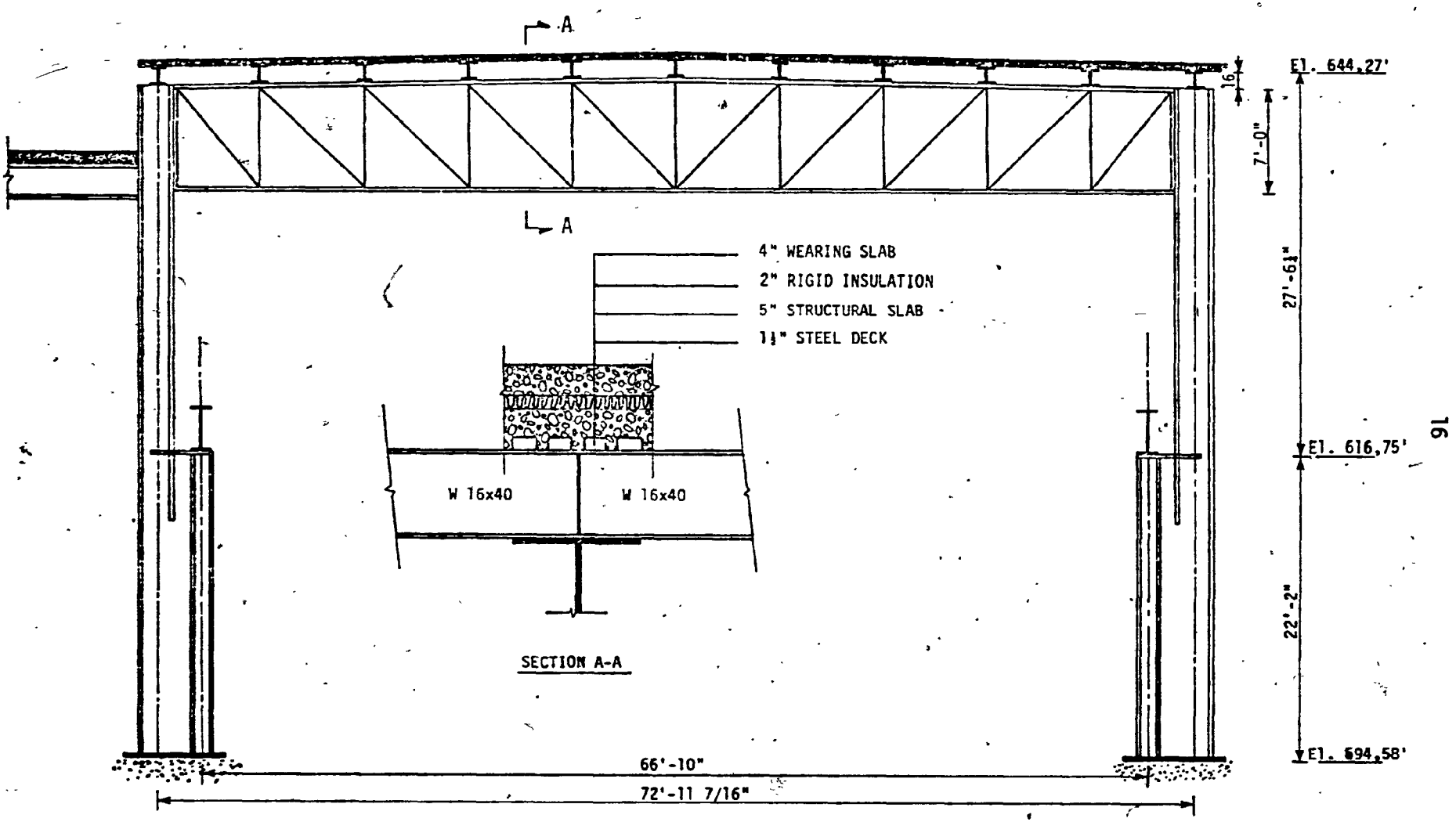

Fig. 2.3 Proposed open-truss super Structure for LG-3 Powerhouse.

summarized as follows:

1- Stability and durability. No apparent deformations due to cracks or permanent deflection should develop even under the most adverse loading conditions developed by the mobile crane.

2- Sufficient thickness is required to provide an adequate structural element, which will be treated hereafter as a plate resting on an elastic foundation; i.e. the insulation material. However, it should be variable in thickness so as to provide the proper slopes and grades for adequate drainage.

Depending on the member being designed, the live load used consisted of either the load applied by the wheels of the mobile crane, or the alternate uniformly distributed snow load. The snow load for this particular location was defined as 80.0 lb/Ft^2.

In the design of both the wearing slab and the steel-composite deck-slab, the uniformly distributed load, i.e. the snow load, never governed because the structural members (ribs) of the composite deck slab were closely spaced (about four feet). The number and position of the individual wheel loads causing maximum moments in the various structural members of the roof are shown in Fig. 2.4. Using the crane manufacturer's manual, one can determine the maximum force applied on the front and back wheels. It was found that a maximum force is subjected on one of the two front tires when an object is being lifted at an angle of approximatly 45^{o} from the centre line of the crane. In such a case, a maximum live

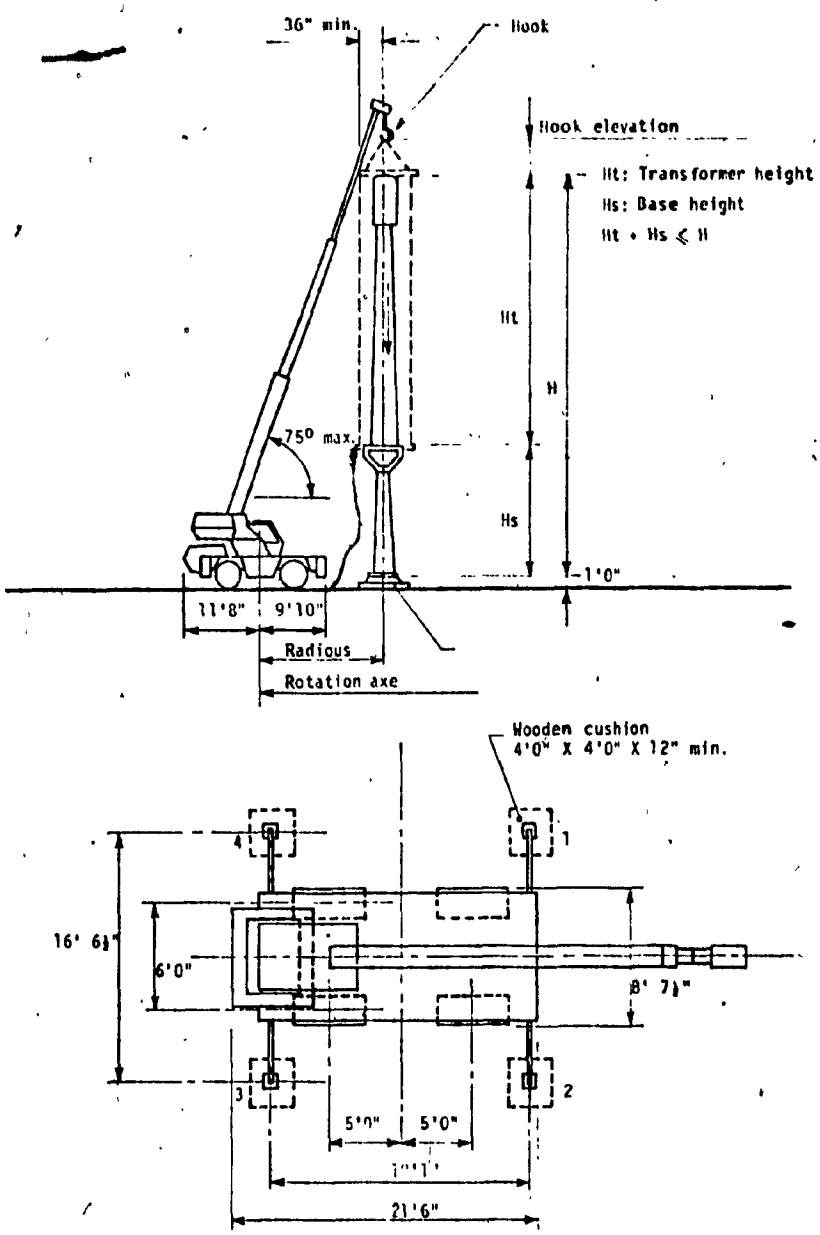

MOBILE CRANE - DROTT 1800								
Load P lb	Boom length Ft	Maximum Radious Ft	Hook Elevatn Ft	Maximum "H" Ft	Outriggers reaction lb			
					1	2	3	4
12500 No Impact	61'-6"	25'-0"	58'-10"	54'-4"	14 706	1 658	14 492	27 540
		30'-0"	54'-6"	50'-0"	14 845	(1 540)	14 348	30 734
12500 + Impact 25%	61'-6"	20'-0"	61'-0"	56'-6"	15 420	3 144	1 527	27 550
		25'-0"	58'-10"	54'-4"	15 590	(662)	15 100	31 355

Fig. 2.4 Mobile crane Load Chart.

load of 28.3 kips was developed.

2.1.2 Boundaries of the Loaded Area

The average actual dimensions of the contact area of each of the two tires is required in order to evaluate the effect of the load applied by the wheels. The unit pressure distribution over the contact area should theoretically be less than or equal to the inflation pressure within the tire. So, by knowing that the tires are inflated to a pressure of 90 lb/in^2 it is possible to determine the dimension of the contact area (Ref. 7) as shown below in Fig. 2.5.

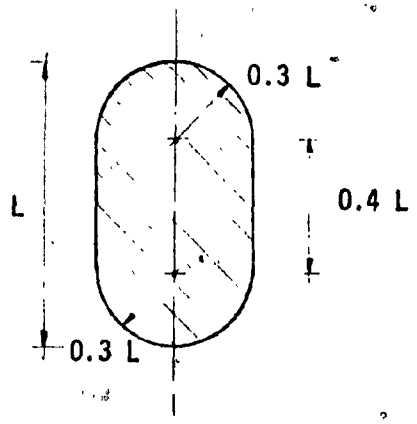

Fig. 2.5 Contact area for the crane tire

$$\text{Contact area "A"} = \frac{28.3 \times 10^3}{90 \times 2} = 157.2 \text{ in}^2 \text{ per tire}$$

Contact area, according to Fig. 2.5 equals

$$\text{"A"} = (0.4L \times 0.6L) + 2\,\frac{\pi}{2}\,(0.3L)^2 = 0.523\,L^2$$

i.e.

$$L = \sqrt{\frac{A}{0.523}} = \sqrt{\frac{157.2}{0.523}} = 17.34 \text{ inches}$$

and;

$$0.6L = 10.4 \text{ inches}$$

2.1.3 Distribution of the Crane Wheel Pressure Over the Wearing Slab

When a distributed crane wheel load is applied to the wearing slab surface through a contact area, there are two fundamental resistances developed. The first, the perimeter shear, is a function of the perimeter of the contact area, and the second, the internal compressive resistance, is a function of the contact area itself.

2.1.4 Design Analysis

The insulation material beneath the wearing slab provides a non-rigid support. The stiffness of the insulation material is relatively low compared to the stiffness of the upper concrete wearing slab, and thus the bending moment in the slab may become quite large in the neighbourhood of a concentrated load.

Several methods may be employed to define the maximum stresses, from which the minimum slab thickness and the necessary reinforcement can be determined. The following calculations describe the methods employed. In the first method the maximum stresses and deflections

were computed for the case where a portion of beam was subjected to a uniformly distributed load.

In the second method, two computer programs were used:

- The Portland Cement Association for Mat-Foundations.
- Finite Element Analysis, using "ANSYS" Program.

2.1.5 Uniformly distributed Load over part of a beam

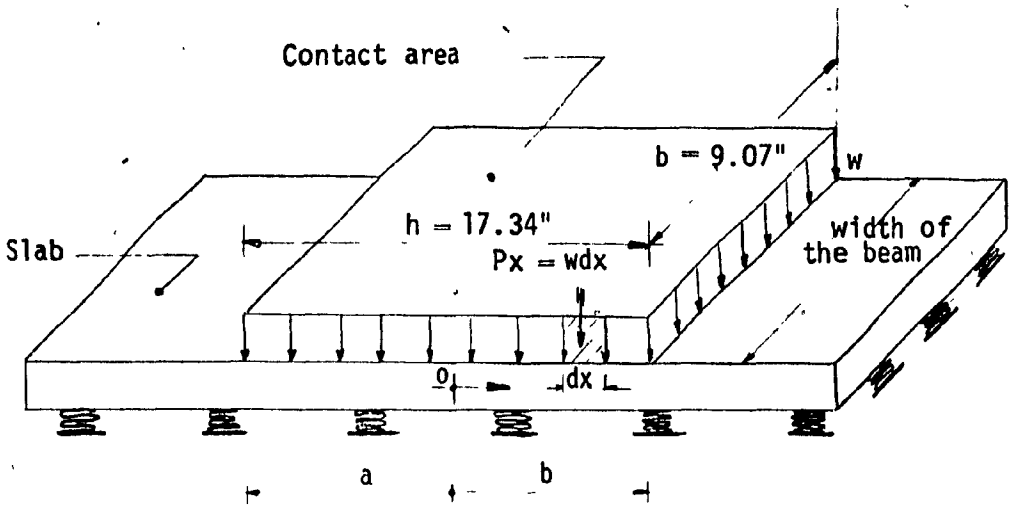

Fig. 2.6 Beam on elastic foundation
(To determine the valves of "h" and "b", see page 24)

As previously noted, the contact area is equal to 157.2 in^2 per tire. It was required to determine the deflection, slope, bending moment and shear in the beam at any section O within the length "h". The section O is located at a distance "a" from the left end of "h" and a distance "b" from the right end of "h" as shown in Figure 2.6.

This problem was solved by assuming that the distributed load is equivalent to a series of closely spaced concentrated loads Px, each of which is equal to wdx, where dx is a diffential length of the beam, Ref. (6).

2.1.6 Deflection

The deflection ΔY, of the point O due to the load $PX = wdx$, as shown in Fig. 2.7, is determined as follow (Ref. 6.),

$$\Delta Y = \frac{\omega\, dx\, \beta}{2K} e^{-\beta x} \quad (\cos \beta x + \sin \beta x) \qquad (2)$$

where "x" is the distance from the load $Px = wdx$ to the point O and "K" and "β" are constants.

The equation of the elastic curve is the familiar $EI \frac{d^2y}{dx^2} = -M$.

In this problem the distribution of the pressure "q" was not known, but since it was assumed to be proportional to the deflection "y", it was advantageous to rewrite the equation as follows by differentiating both sides of the equation twice. The result found was,

$$EI \left(\frac{d^4y}{dx^4}\right) = \frac{-d^2M}{dx^2} \qquad (3)$$

But $$\frac{d^2M}{dx^2} = q$$

This fact may be shown as follows. In Fig. 2.7.b the forces acting on a block of differential length dx cut from the beam are shown.

By applying the equilibrium equation $\Sigma F = 0$ to those forces and neglecting the product of differential terms, the following relationship was found:

$$\frac{dv}{dx} = q \quad \text{but} \quad V = \frac{dM}{dx}, \text{ i.e } \frac{d^2M}{dx^2} = q$$

Therefore equation (3) may be written:

$$EI\left(\frac{d^4y}{dx^4}\right) = -q \tag{4}$$

If "q" in equation (4) is expressed as a function of the deflection "y", the equation can be then integrated.

Since the continuous support (the insulation material) is elastic, the pressure "w" per unit length may be expressed as;

$$q = W = bK_0y \tag{5}$$

where: "b" is the width of the bottom of the beam, and

"K_0" is the spring constant of the elastic support, i.e. it is the force exerted by the elastic support per unit deflection of the support. The manufacture's specs indicate that a strain of 5% occurs when a load of 30 p.s.i. is applied to the surface of the insulation. Since we are using a total thickness of 2.0 inches, K_0 can be determined as follows:

$E = \frac{\Delta t}{t} = 0.05$

$t =$ 2.0 inches

$\Delta t =$ 0.1 inches, (i.e. 2 X 0.05 = 0.1 inches)

$K_0 = \frac{30}{0.1} = 300$ lb/in^3 or lb per in^2 per inch

Also: $K = b K_0$ (6)

Therefore: $q = K y$ (7)

where; "K" is defined as the spring constant per unit length of the elastic support.

It should be remembered that "K" includes the effect of the width of the bottom of the beam and will be numerically equal to "K_0" only when the beam is of unit width; i.e;

The contact area = 157.2 in^2

If "h" = 17.34 inches, "b" should be = $\frac{157.2}{17.34}$ = 9.07 inches

$K = 9.07 \times 300 = 2721.0$ lb/in^2

The substitution of $q = Ky$ in equation (4) gives;

$$EI \left[\frac{d^4y}{dx^4}\right] = -Ky \quad (8)$$

which is the differential equation of the elastic curve of any beam on an elastic support. For a long beam, two of the four terms are equal to zero and the final solution is;

$$y = e^{-\beta x} \quad (C_1 \cos \beta x \pm C_2 \sin \beta x) \quad (9)$$

where;

$$\beta = \sqrt[4]{\frac{K}{4EI}}$$

and the dimensional unit of "β" is L^{-1} where "L" is the dimension of length.

Assume that the thickness of the slab is four (4) inches, i.e.

$$I = \frac{bd^3}{12} = \frac{9.07 \times 4^3}{12} = 48.4 \text{ in}^3$$

i.e. $$\beta = \sqrt[4]{\frac{2721.0}{4 \times 3 \times 10^6 \times 48.4}} = 0.0465$$

Now after determining the values of K and β, the resultant deflection "y" of the point 0 caused by the total distributed load will be equal to the algebraic sum of all the values of Δy for each of the loads wdx, as given by the equation (2). As there are infinite number of loads wdx on both sides of the point 0 ($x = o$), the following two integrals are required to sum up the values of Δy :

$$y = \Sigma \Delta y = \int_o^a \frac{wdx}{2K} \beta e^{-\beta x} (\cos \beta x + \sin \beta x)$$

$$+ \int_o^a \frac{wdx}{2K} \beta e^{-\beta x} (\cos \beta x + \sin \beta x) \quad (10)$$

Equation (10), when integrated gives the value of the deflection at point 0 as :

$$y = \left[\frac{w}{2K}\right] (2 - e^{-\beta a} \cos \beta a - e^{-\beta b} \cos \beta b) \quad (11)$$

It is noted that y is a maximum when $a = b = \frac{h}{2} = \frac{17.34}{2} = 8.67$ inches

i.e.; $\beta a = \beta b = 0.0465 \times 8.67 = 0.403$

$$w = \frac{28.3 \times 10^3}{2 \times 17.34} = 816.0 \text{ lb per unit width}$$

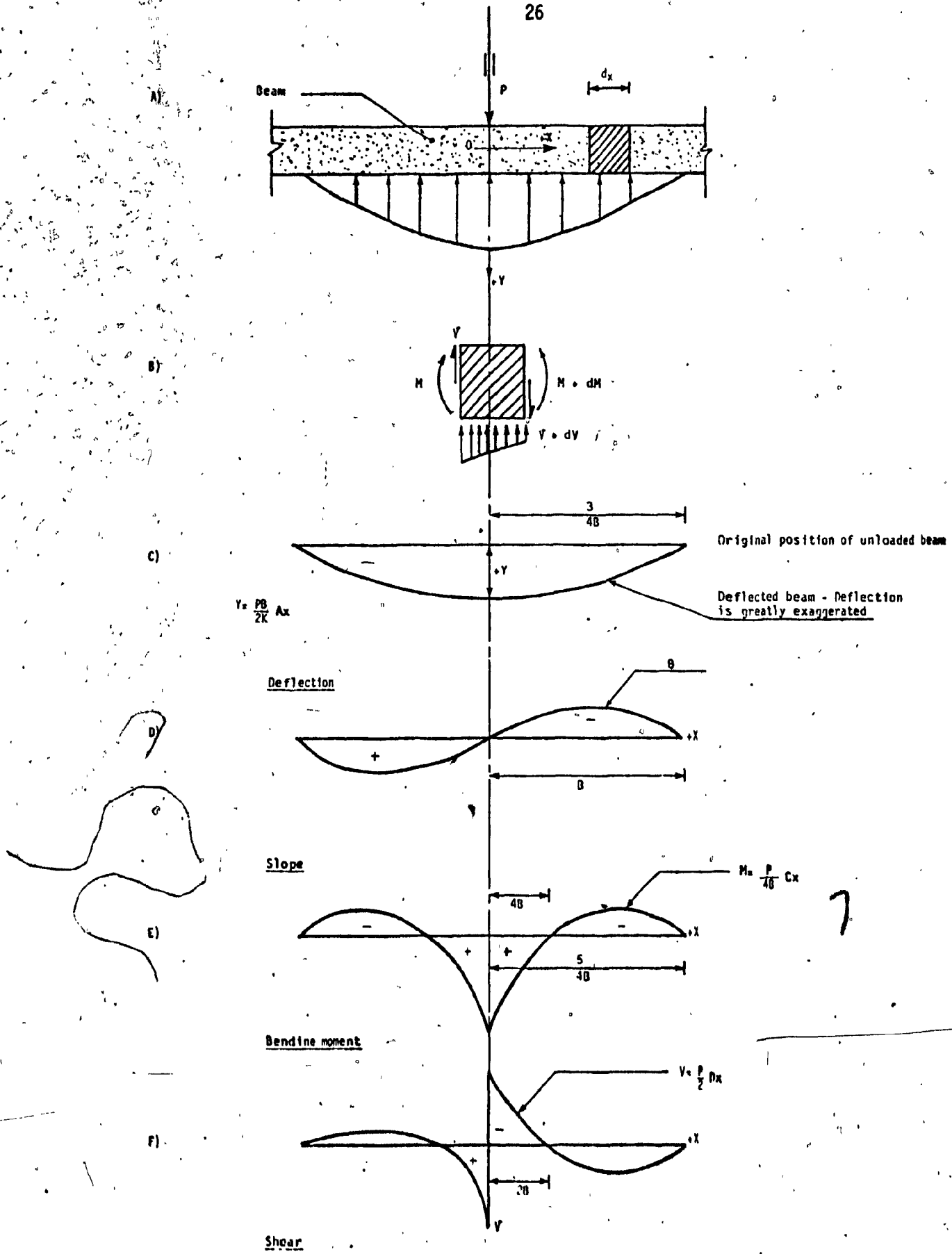

Fig. 2.7 Deflection, slope, bending moment and shear in beam in continuing elastic support.

Substituting w in equation 11, we obtain

$$y_{max} = \frac{816.0}{2(2721.0)} \left[2 - 2(e^{-0403} \cdot \cos 0.403)\right]$$

$$= 0.0995 \text{ inches}$$

2.1.7 Maximum Bending Moment

The location of the point O which will be under the maximum bending moment, M, can be determined according to the following equation:

$$M = \left(\frac{w}{4\beta^2}\right) (B_{\beta a} + B_{\beta b}) \qquad (12)$$

If the loaded length of the slab is short, that is, if h is less that $\frac{\pi}{2\beta}$ the maximum bending moment occurs at the mid-point of the distributed load. If h is greater than $\frac{\pi}{2\beta}$, there are two locations within the length h which give the same maximum moment. These two points are assumed to be at a distance of $\frac{\pi}{4\beta}$ from each end of the distributed load.

$$h = 17.34 \text{ inches}$$

$$\frac{\pi}{2\beta} = \frac{3.14}{2 \times 0.0465} = 33.78 \text{ inches}$$

i.e. $h < \frac{\pi}{2\beta}$ one point at mid distance of h

But, $a = b = 8.67$ inches and $Ba = Bb = 0.403$

also: $Bx = e^{-x} \sin x$

i.e. $B_{\beta a} = B_{\beta b} = e^{-0.403} \sin 0.403 = 0.262$

$$M(max) = \frac{816.0}{4(0.403)} \times 2(0.262) = 49448.3 \text{ lb.in}$$

$$= 4.12 \text{ Feet-kips}$$

2.1.8 Computer Analysis

2.1.8.1 Mat Foundation Program - Portland Cement Association

In this program the slab is analysed using thin plate bending theory and the finite element method. The slab is assumed to behave like a thin plate in bending, and the material underneath is assumed to behave like a set of isolated springs (Winkler foundation). The loads, which are usually transmitted to the slab from the columns, are in this case applied by the contact area of the mobile crane tires.

A plastic analysis of the mat is made under ultimate loads. These loads are applied only at the nodes of the finite element mesh. If any loads happen to exist within an element they must be distributed to the adjacent nodes. The column dimensions, or in this case the contact area, must also be distributed to these nodes in the same proportions as shown in Fig. 2.8. A 14" x 14" element has been adopted to develop the mesh illustrated in Fig. 2.9. The diagrams on page 31 Fig. 2.10 show the results obtained and the location of the maximum deflection and bending moments.

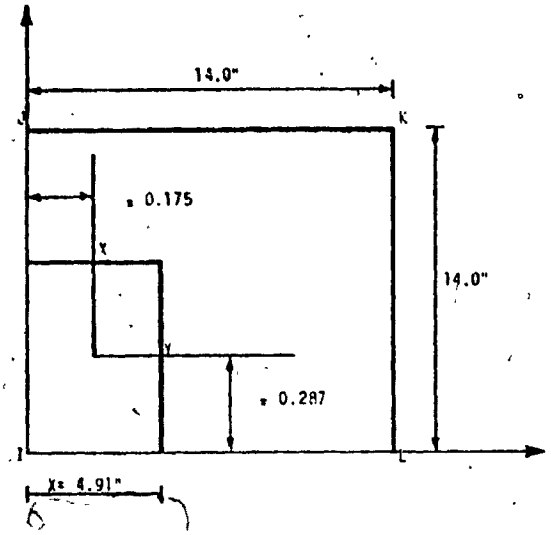

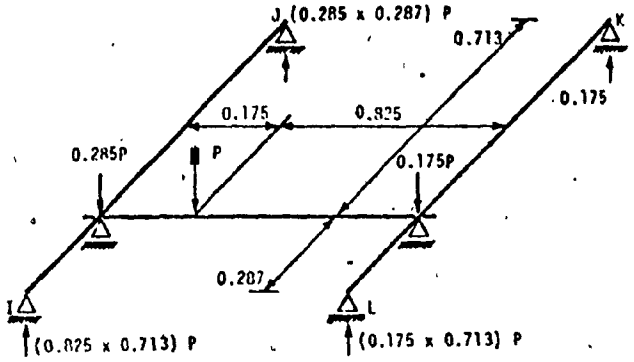

$= \frac{2.455}{14.0} = 0.175$

$= \frac{4.0}{14.0} = 0.287$

Node	Column size X	Y
I	(0.825X	0.713Y)
J	(0.285X	0.287Y)
K	(0.175X	0.287Y)
L	(0.175X	0.713Y)
	1.0X	1.0Y

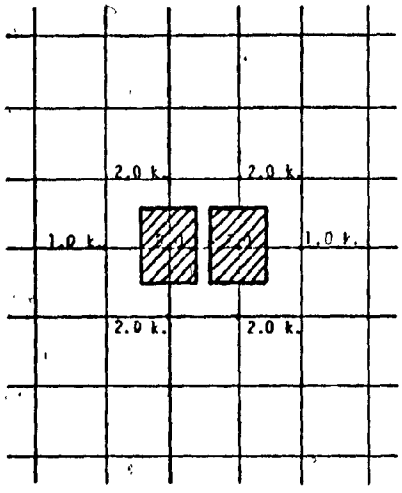

NODE	X	Y
50	0.38	0.29
51	0.38	0.29
64	0.07	0.48
65	0.75	1.44
66	0.75	1.44
67	0.07	0.48
80	0.38	0.29
81	0.38	0.29
	3.16ft	5.0ft

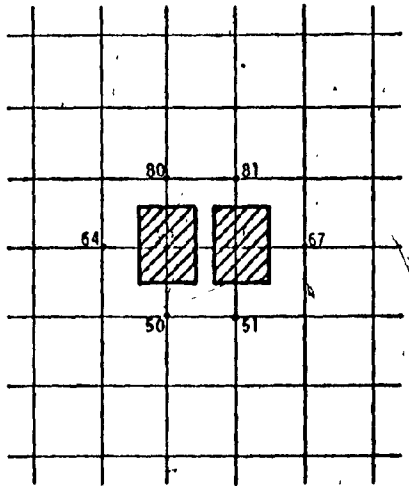

Total load: 28.0 Kips

Total perimeter: 16" X 4" + 9.82" X 4": 103.28"

Fig. 2.8 Distribution of tire load and contact area.

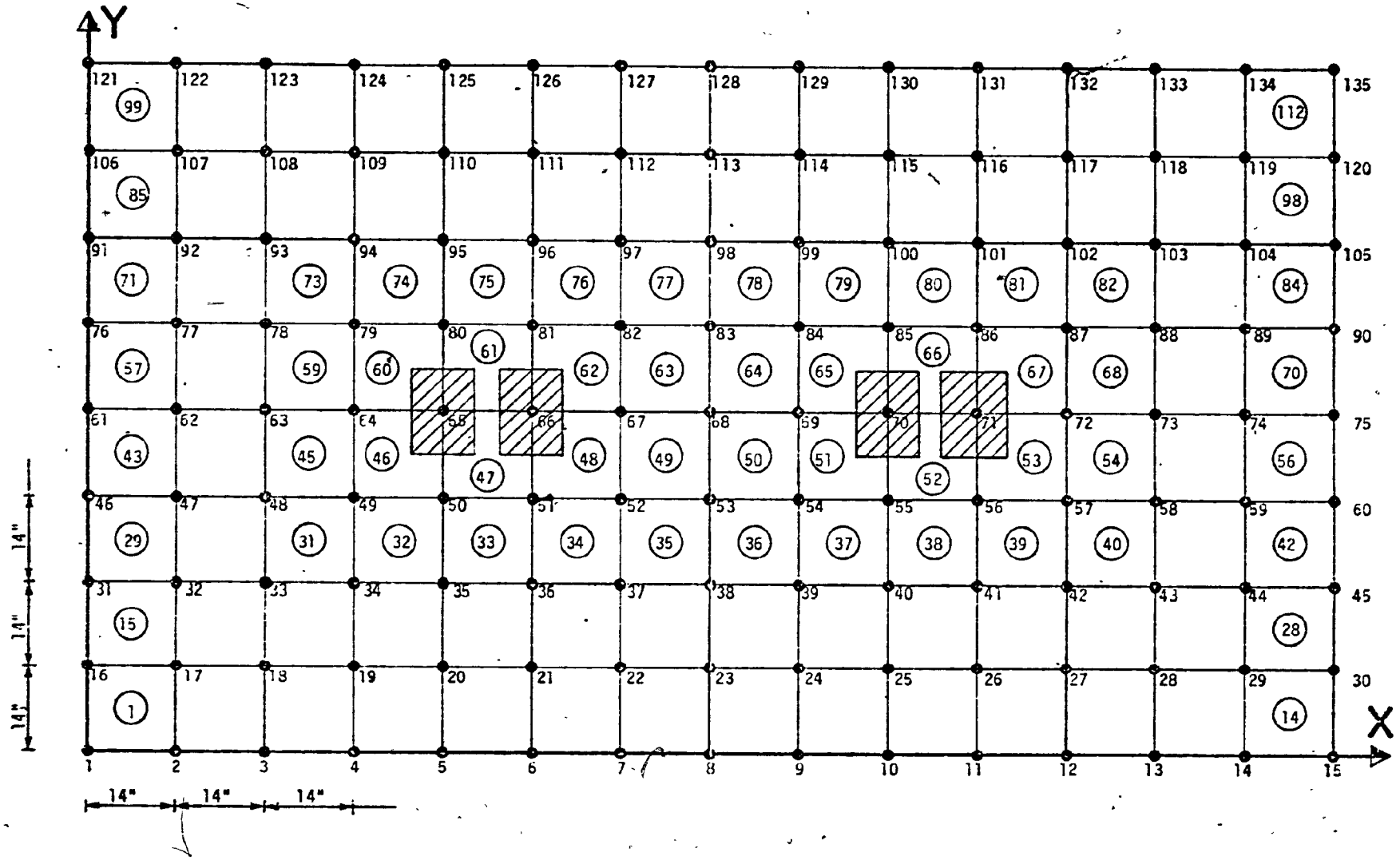

Fig. 2.9 Mat Foundation Program - P.C.A.

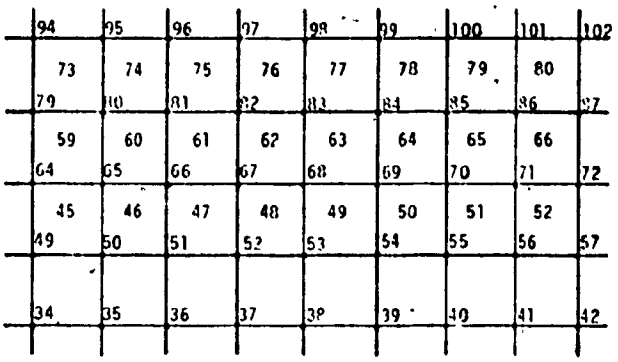

Node #	64	65	66	67	68	69	70	71	72
Line 1									
Deflection:	0.02"	0.027"	0.029"	0.025"	0.023"	0.025"	0.027"	0.027"	0.019"
Contact pressure: K/FE^2	0.44	0.59	0.62	0.55	0.50	0.53	0.59	0.56	0.41

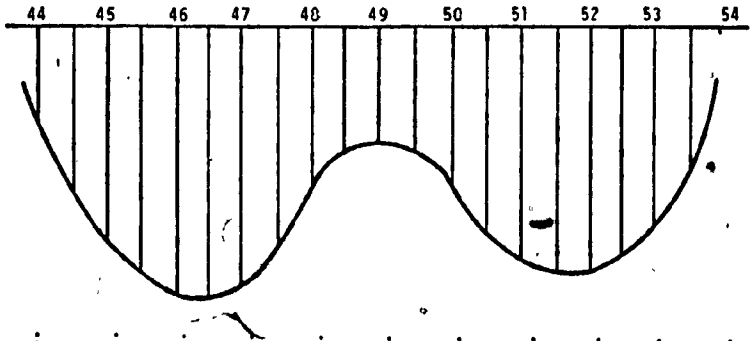

My: Ultimate	1.577'k.	3.109'k.	5.700'k.	5.821'k.	3.345'k.	2.411'k.	3.320'k.	5.747'k.	5.642'k.	2.971'k.	1.477'k.
My:	0.927	1.828	3.35	3.42	1.967	1.42	1.95	3.38	3.29	1.74	0.83

Fig. 2.10 Deflection and bending moments results - PCA Program.

2.1.8.2 Finite Element Analysis - ANSYS Program

An elastic flat rectangular plate is the element which has been choosen for the above mentioned program. Each element has pure bending capabilities and three degrees of freedom at each of its four nodes.

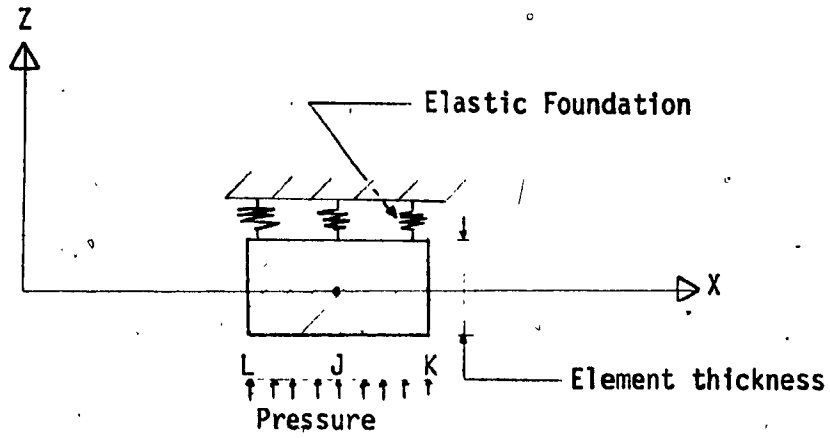

Fig. 2.11 Element used in ANSYS Program

The geometry, nodal point locations, loading and coordinate system for this element are shown in Fig. 2.11. The element is defined by four nodal points, four thicknesses (which are all equal in the present case), and its material properties.

An elastic foundation stiffness will be included in the element formulation. This value is defined as the pressure required to produce a unit normal deflection of the foundation. The actual locations of the front tires of the mobile crane on the finite element mat are shown in Fig. 2.12. This distribution has been altered to the one shown in Fig. 2.13 in order to be suitable for use in this program. Fig. 2.14 shows the actual model used in analysing the slab behaviour, and the results of this analysis.

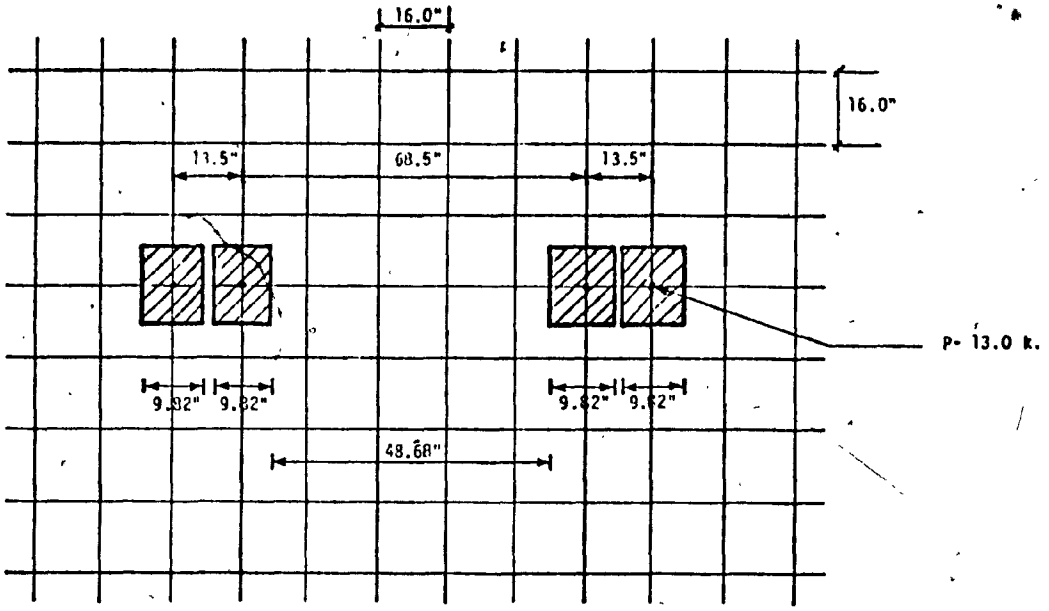

Fig. 2.12 Actual locations of front tires.

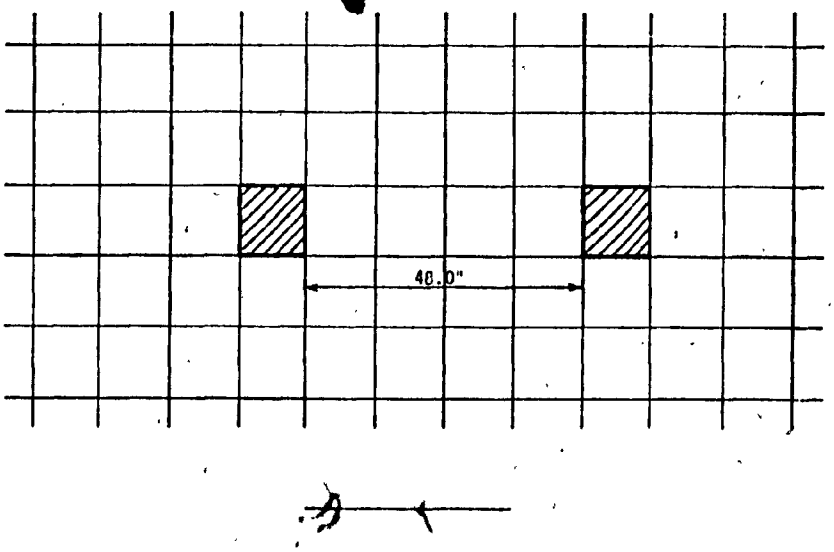

For two tires ; P_u= 26.0 k, contact area= 157.3 X 2 in ^{2}= 314.6 in^2

Element area: 16.0 X 16.0= 256.0 in^2

$w = \frac{26.0}{256.0} = 101.6 = 102$ lb

Fig. 2.13 Altered distribution of tire load and contact areas.

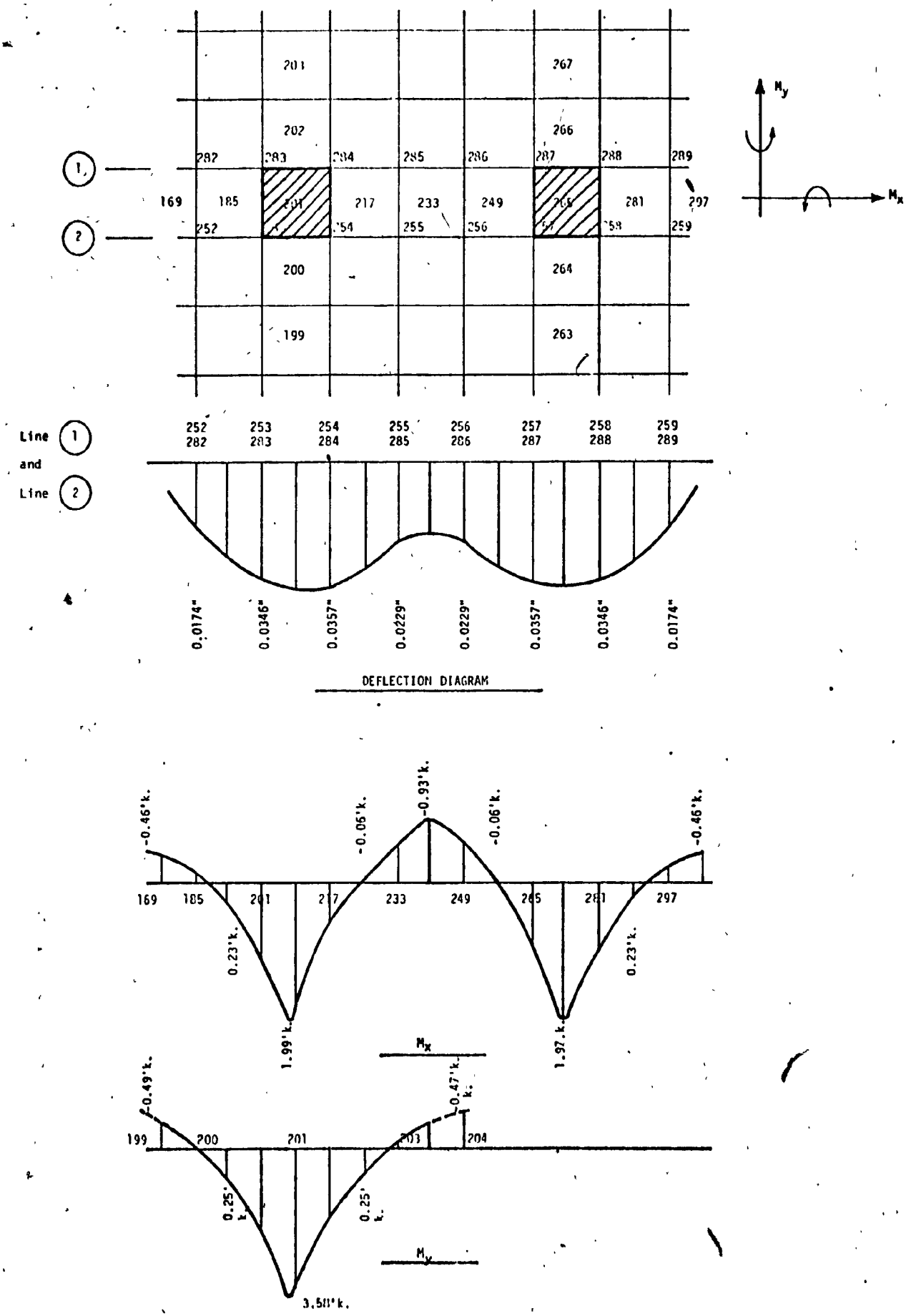

Fig. 2.14 - Deflection and bending moments results - ANSYS Program.

2.1.9 Conclusion

The following Table 2.1 shows the different values of deflection and bending moment that resulted from the calculations obtained by analysing the slab as a partially loaded beam, and from the two computer programs.

Table 2.1;

Comparative table of Deflection and Bending Moment values.

Method used	Deflection (in)	Bending Moment (Ft.K.)
(1) A uniformly distributed load over part of beam.	0.0995	4.12
(2) As Mat Foundation using Portland Cement.	0.029	3.42
(3) Finite Element using ANSYS Program.	0.0357	3.581

From the results, it should be noted that in the first method with the applied load distributed over part of the beam, the values for both the deflection and the bending moments were the greatest. However, when plate action was considered in the second and third methods the resulting values are substantially lower.

2.1.10 The Structural Slab and its Steel Supporting Elements

Once the depth of the protection slab was determined, the structural composite slab thickness and reinforcement were calculated using the conventional method.

All possible combinations of the basic load conditions were applied in order to determine the dimensions and properties of steel supporting elements.

2.2 Alternative no. 2

In this alternative, special attention was given to the water-tightness of the roof. Further study and investigation led to the idea of using a series of steel panels to cover the whole surface. Basically the same concept was used in a roof system of a nuclear power plant where the reactor building had to be air tight so that radiation would not escape into the atmosphere. Obviously the cost of such a structure exceeds by a considerable margin the cost of the conventional roof system mentioned in alternative no. 1. However, in a location as remote as LG-3, given the severity of the climate, the maintenance costs over the years would also be a significant factor in deciding the best solution. Hence, the water tightness is assured by a ¼ inch thick steel plate with tee stiffeners on its underside. The plate is made composite with the six inch thick concrete slab by means of shear connectors so that the structure behaves like a composite orthotropic roof as shown in Fig. 2.15.

The design of the protection slab was kept the same as in alternative no. 1, but in order to reduce the overall dead load on the

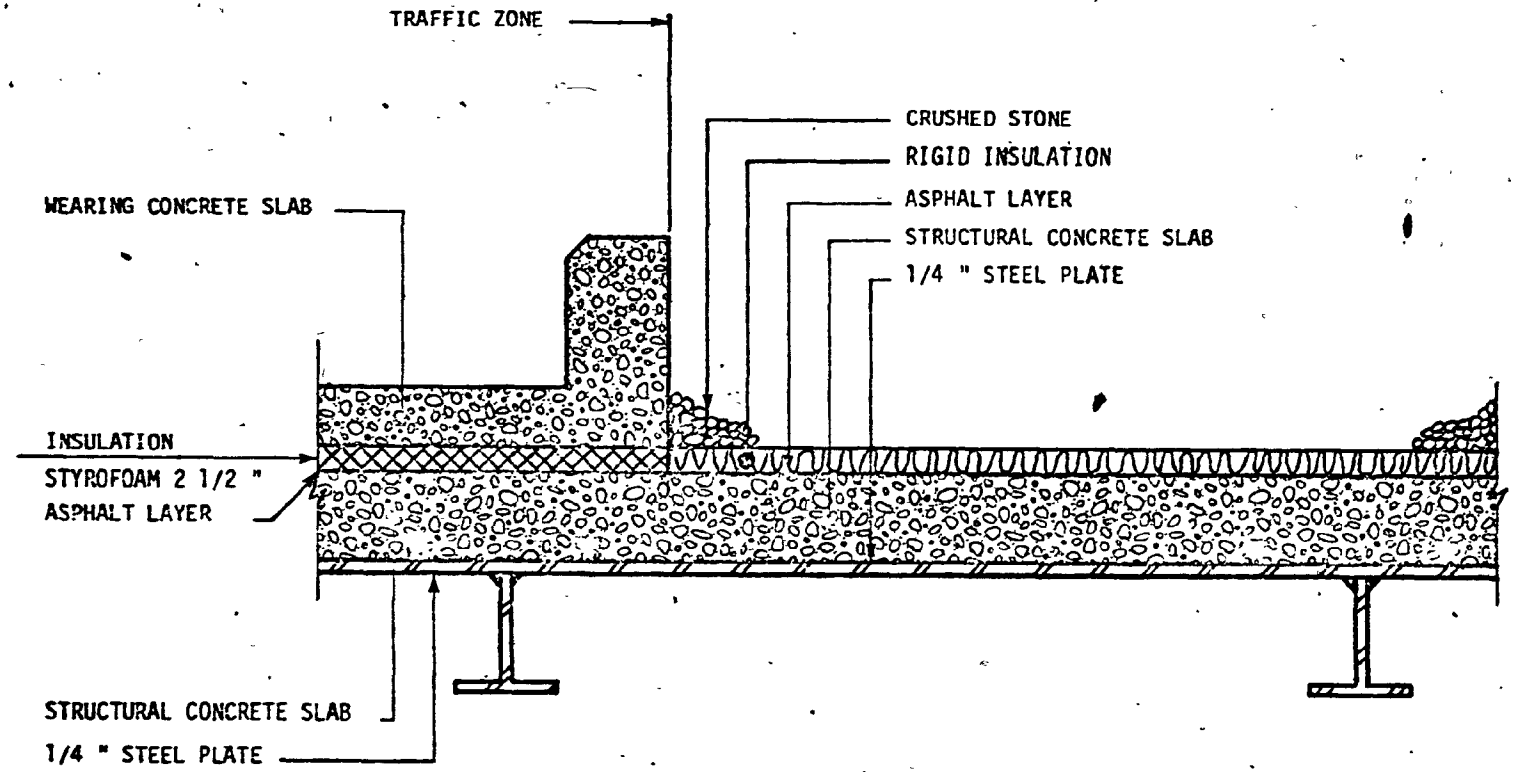

Fig. 2.15 ALTERNATIVE Nº 2

roof, the use of the protection slab was limited to the traffic zones and to areas where equipment was to be handled and or installed. Those areas free of traffic were covered with crushed stone. The structural concrete slab was covered with an asphaltic emulsion and then with a layer of thermal insulation.

It is interesting to note at this point that two alternatives were considered concerning the use of the orthotropic steel plate. One approach was calling for a thicker steel plate without any concrete cover. This solution would required more tee stiffners and the plate would be almost a typical steel-deck bridge design. On the other hand, the idea of combining the concrete and the steel plate to acquire more rigidity was also popular. A typical panel was designed for each of the two alternatives, and a selected specialized manufacturer was asked to provide an estimate of the fabrication costs of each panel. Without taking into consideration the costs of concreting the structural slab, the total cost of fabricating a steel-only roof panel was 64% higher than steel-concrete panel.

2.2.1 Design of the Deck Plate

To enable an approximate computation, the deck plate supported by the open-rib-stiffeners was treated as an isotropic plate, continuous in the Y direction (Fig. 2.16) over the ribs which act as simple unyielding supports.

It was first assumed that the weight of a 6 inch layer of fresh

concrete combined with a live load of 20 lb/ft^2 is supported by a plate strip having a width of one foot and is distributed uniformly over several spans.

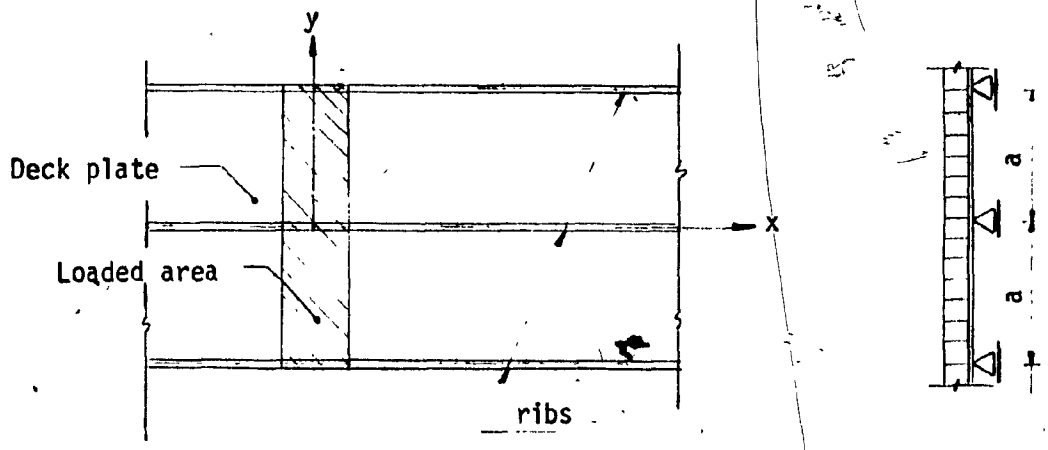

Fig. 2.16 Loading of the deck-plate

The bending moments and deflection would then occur predominantly in the Y-direction and could be approximately computed with the continuous beam formulae. In the actual case, the plate extends in the x- direction beyond the width of the applied load and the portions of the plate on either side of the load also participate in the stresses. Thus, the critical maximum moment in the Y-direction in the one foot wide plate strip under the centre of the applied load will be smaller in the full plate than in the plate strip of the first case when the plate was treated as a continuous beam. The required spacing between the ribs was found to be 4 ft., and the required plate thickness, 1/4 inch, (including 1/16 inch provided for corrosion).

2.2.2 Design of the Open Rib Beam

Usually in a computation procedure for an orthotropic deck with open ribs, the calculation is made in two steps. In the first step the bending moments in the longitudinal ribs and in the floor beams are computed under the assumption that the floor beams are rigid. In the second step the effects of the elastic flexibility of the floor beams are determined.

In the present case the floor beams are replaced by the main girder of the rigid frame. The rigidity of the latter is greater than that of the T-Stiffeners. Therefore in view of the rigidity of the main girders it was decided that no further computations were necessary in order to correct the bending moments obtained.

For orthotropic bridge deck design, the truck wheel loads are considered the principal live load (Ref. 1). Such was also the case in the present study. The mobile crane loads already mentioned in the design of the protection slab were used rather than the uniform snow load. The ribs were calculated for a maximum axial loading of 28.3 kips. Due to the presence of the concrete protection on top of the structural slab, the contact area of the steel deck plate is enlarged due to the assumption that the load is distributed downward at a 45^{o} angle in all directions, as indicated in Figure 2.17.

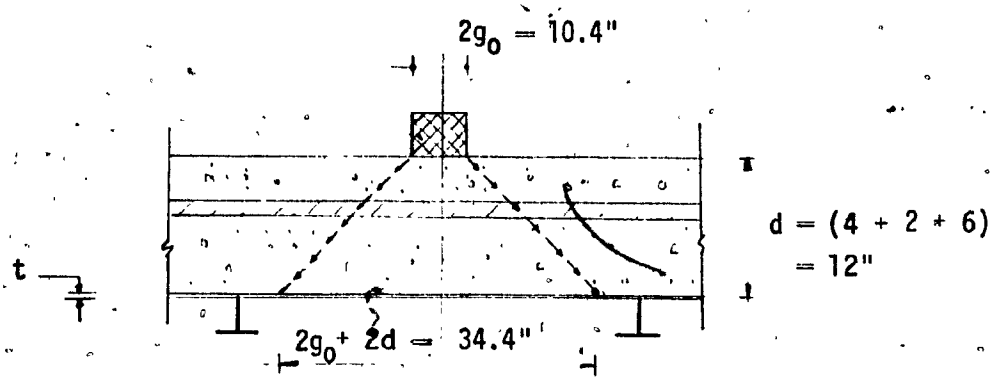

Fig. 2.17 Distribution of tire load through the slab

The bending moments and reactions of the ribs are determined by applying the influence lines of a continuous beam. A separate T-rib is considered as a continuous beam over multiple equal spans supported by the main girders of the rigid frames. The beam is assumed to be loaded only in the middle span by the concentrated wheel load as indicated above.

In determining the "section properties" of T-rib section, where the plate acts as the upper flange of a T-beam, the effective width of the flange must be calculated.

In general, the effective width could be smaller, greater, or equal to the rib spacing. It depends principally on the type of loading and on the relation between ribs and floor beam (main girder) spacing.

As established in Ref. 1, it is first necessary to determine the so-called "effective span" of the rib which is defined as the average length of the positive moment area of the rib. In our analysis,

it was found that the effective span of the ribs has the approximate value;

$$L_e = 0.7\ L \quad \text{and for} \quad L = 23.67\ \text{Ft.}$$

$$L_e = 16.57\ \text{Ft.}$$

From Figure 2.18, the ideal rib spacing is found out to be:

$$\frac{B}{a} = \frac{34.4"}{48.0"} = 0.716$$

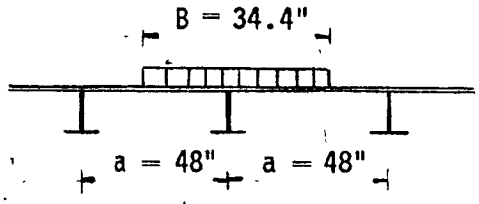

Fig. 2.18 Effective width of the rib-beam

Using Diagram no. 3, published in Ref. 1; under case of loading no. 1 as shown on page no. 43.

$$\frac{a^*}{a} = 1.92$$

Hence; the ideal rib spacing $a^* = 92.16$ inches

Therefore the value of the coefficient β, published in Ref. 1; shown in page no. 44 is;

$$\beta = \frac{\pi\ a^*}{L_e} = 1.456$$

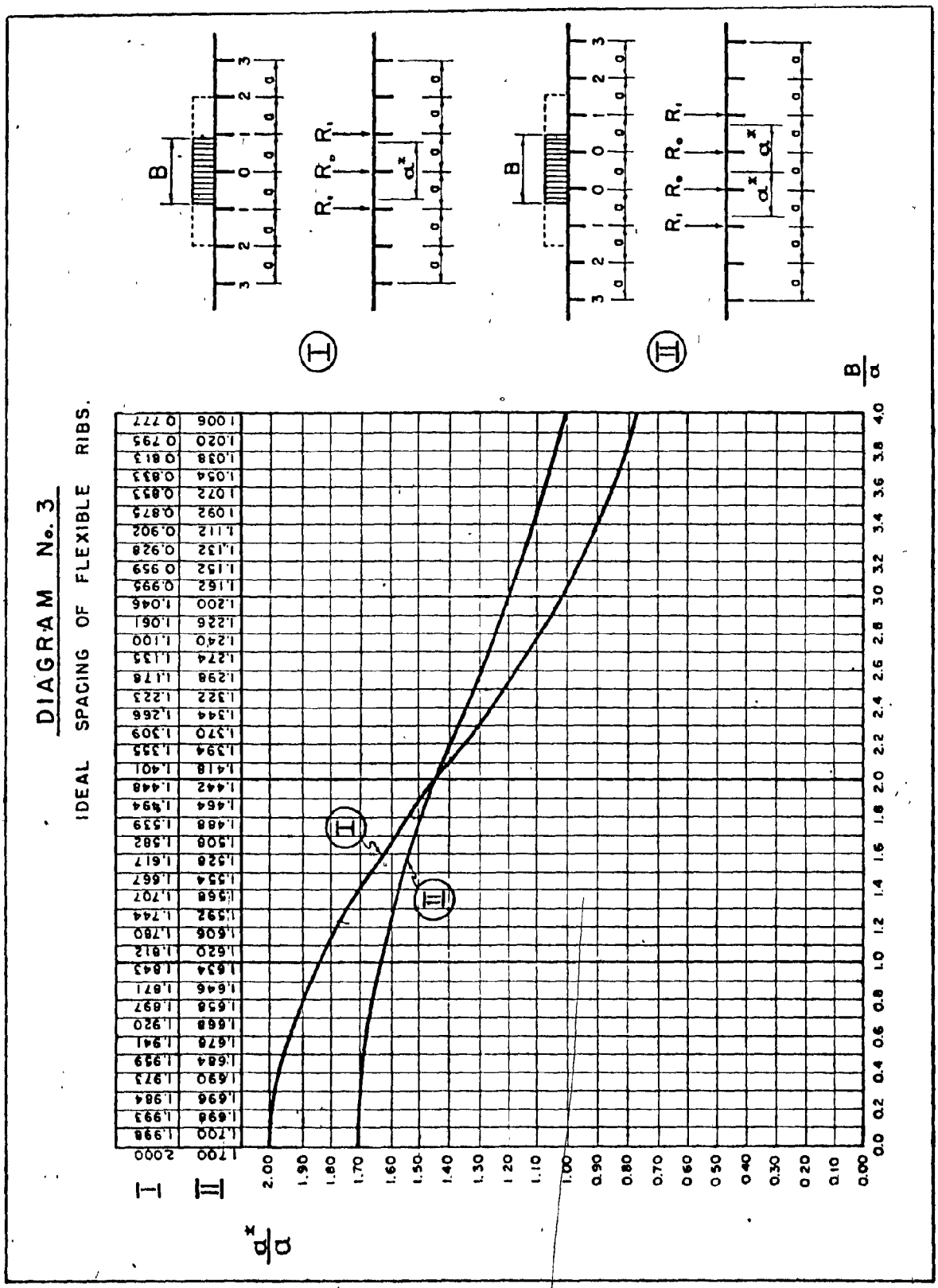

I	II
2.000	1.700
	1.998
	1.993
	1.984
	1.973
	1.959
	1.941
	1.920
	1.897
	1.871
	1.843
	1.812
	1.780
	1.744
	1.707
	1.667
	1.617
	1.582
	1.539
	1.494
	1.448
	1.401
	1.355
	1.309
	1.266
	1.223
	1.178
	1.133
	1.100
	1.061
	1.046
	0.995
	0.959
	0.928
	0.902
	0.873
	0.833
	0.813
	0.795
	0.777

DIAGRAM No. I

EFFECTIVE WIDTH OF THE ORTHOTROPIC DECK PLATE.

a_o AND l_o = EFFECTIVE WIDTH OF THE DECK PLATE.

a^* AND l^* = IDEAL SPANS OF T-RIBS, BOX-RIBS OR FLOOR BEAMS.

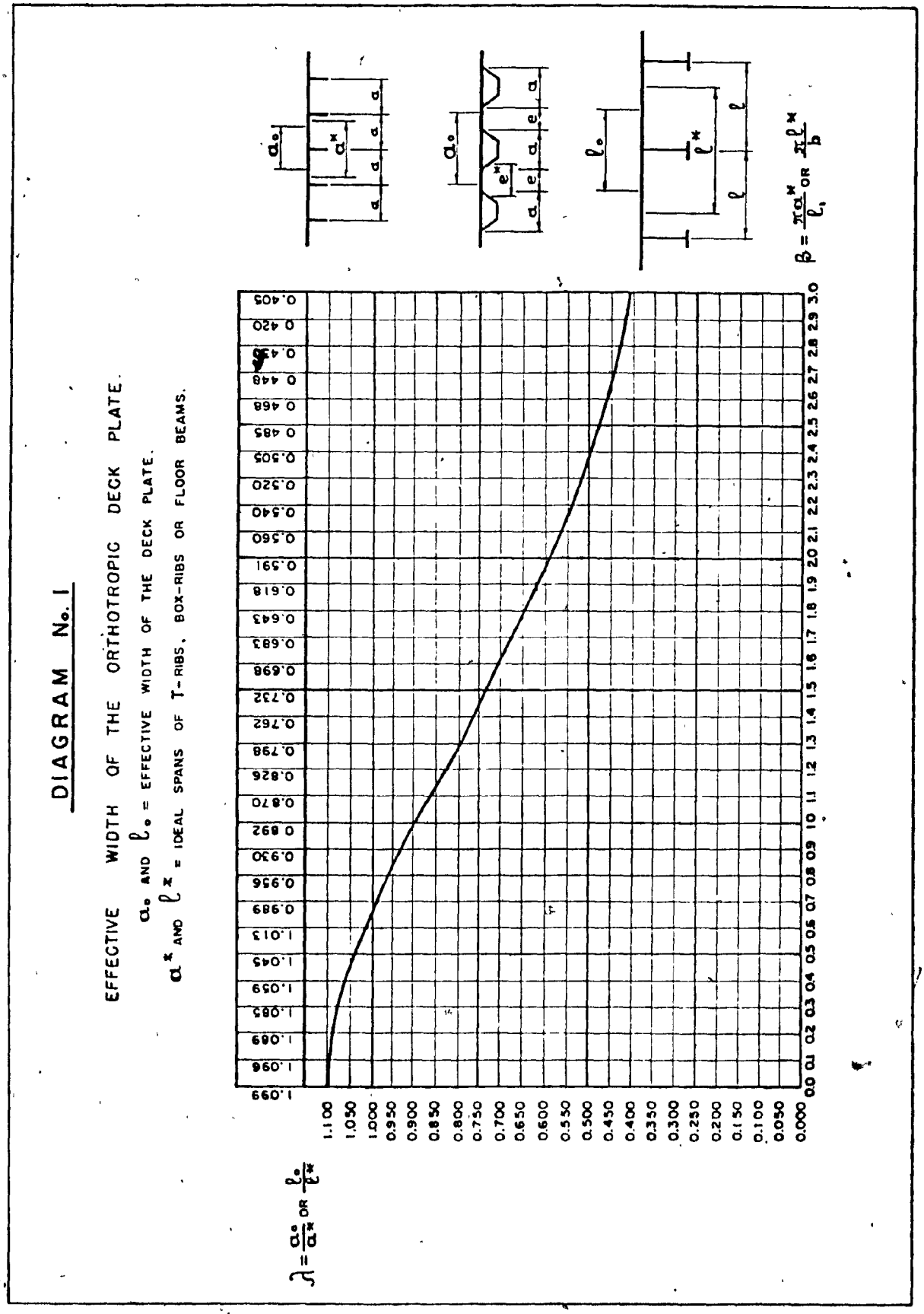

From the Diagram no. 1 on page 44 , the effective width of the plate acting with the directly loaded ribs; (Ref. I)

$$a_o = \left(\frac{a_o}{a^*}\right) a^* = 0.75\ a^* = 69.12 \text{ inches}$$

From the effective width, the section properties of one T-rib are determined and the maximum positive and negative bending moments are then calculated. The composite action between the concrete slab and the ribbed deck is considered in the areas of the positive moments while the section properties of the deck and rib alone are considered on the areas of the negative moments. A WT 9 x 22.5 was found to be adequate as a rib under all loading conditions.

2.3 Alternative no. 3

Alternative no. 3 consists of the same basic roof as in alternative no. 2 except that the thermal insulation would be below the steel deck and the six inch concrete slab would be covered by a two inch wearing slab, as shown on Fig. 2.19. This alternative was considered due to the growing concern about the durability of the insulation material if it were placed between two layers of concrete. Water was due to infiltrate through to the insulation sooner or later, and the long term effect of this trapped humidity, especially when the temperature dropped significantly, on the wearibility of the insulation had to be considered.

It was proposed that insulation be installed on the underside

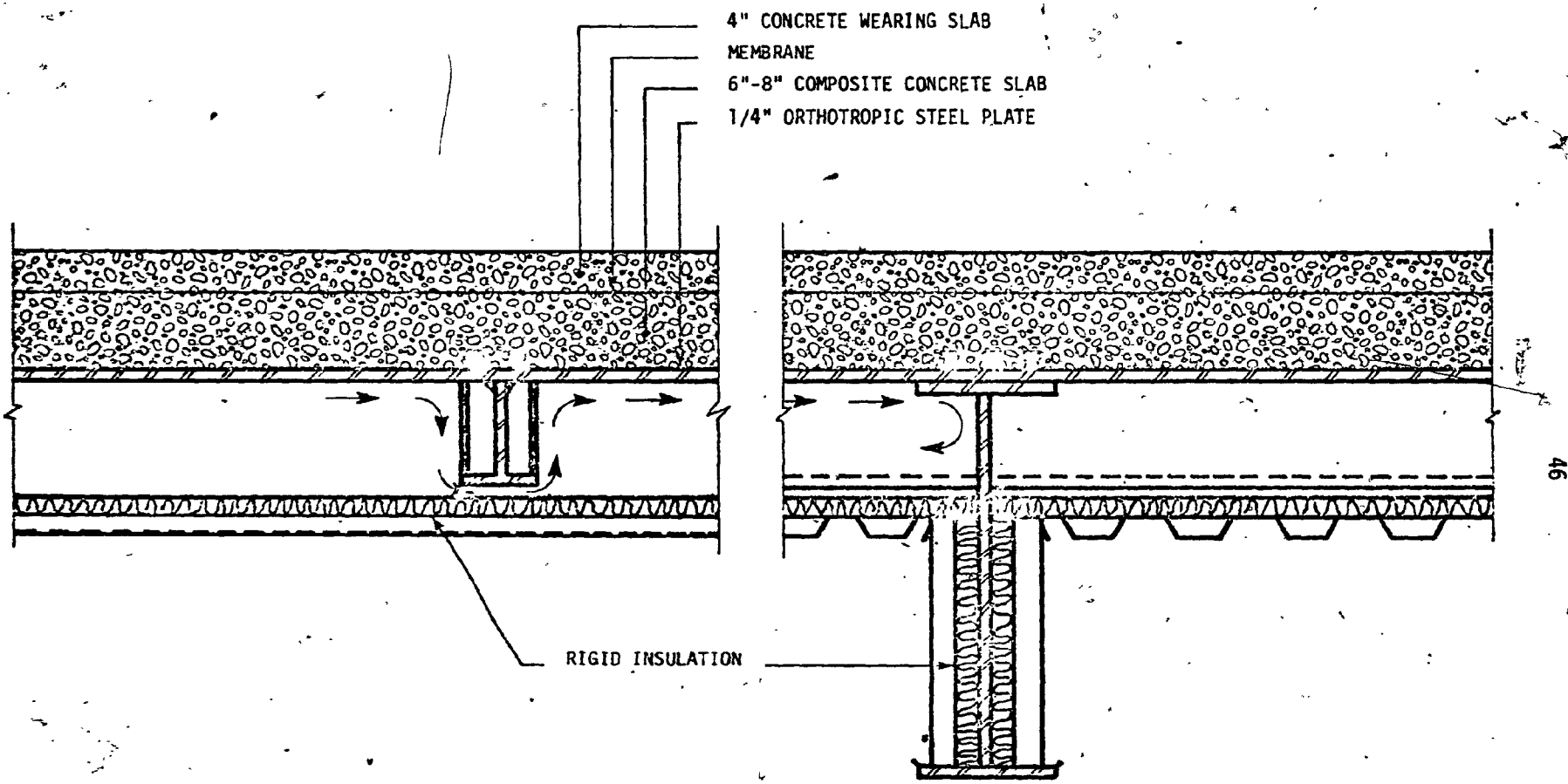

Fig. 2.19 ALTERNATIVE Nº 3

of the steel deck and on both sides of the ribs and main girders. However two drawbacks of this system were determined; the first was the problem of condensation which would certainly occur in the winter season when the inside temperature would be much higher than the outside one. The second ; from the architectural point of view it was difficult to find a type of insulation that would have an acceptable appearance and would still be relatively inexpensive and easy to install.

CHAPTER 3

CONSTRUCTION DETAILS AND EXECUTION

Following a lengthy debate of the three previous alternatives, several economic analyses were prepared to facilitate their comparison. Meanwhile more data was obtained on the crane load which was to represent the principal live load on the roof. Finally the solution detailed in Figs 3.1 and 3.2 was selected and the necessary elaborate calculations were completed to insure the safety of the structure.

One significant modification that can be noted in this final approch was the addition of the corrugated sheets on top of the insulation material. The purpose of those sheets is to permit air to circulate, and hence reduce the effect of dampness on the insulation. With regard to the live load produced by the mobile crane, a maximum vertical force of 31.35 kips, including an impact factor of 25% was employed in the final calculations. The load would be applied on the top of the concrete slab by the outriggers of the crane, each of them having contact area of four square feet. (2 Ft x 2 Ft). Further research was also conducted in order to determine the actual percentage of wheel load that would be directly placed on an individual rib. Following a computer analysis, it was found that this load was equal to 0.7P, where "P" is the maximum vertical load. The remaining force would be distributed to the adjacent ribs.

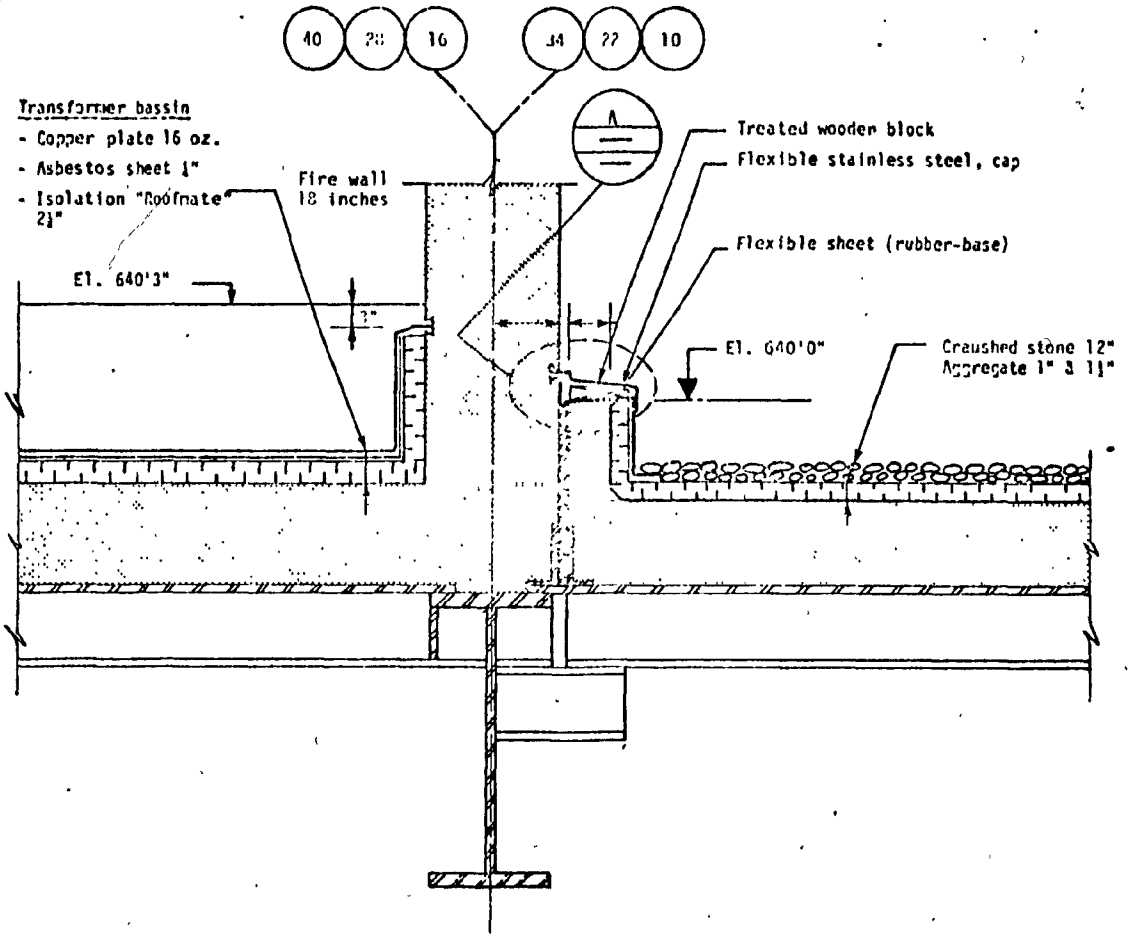

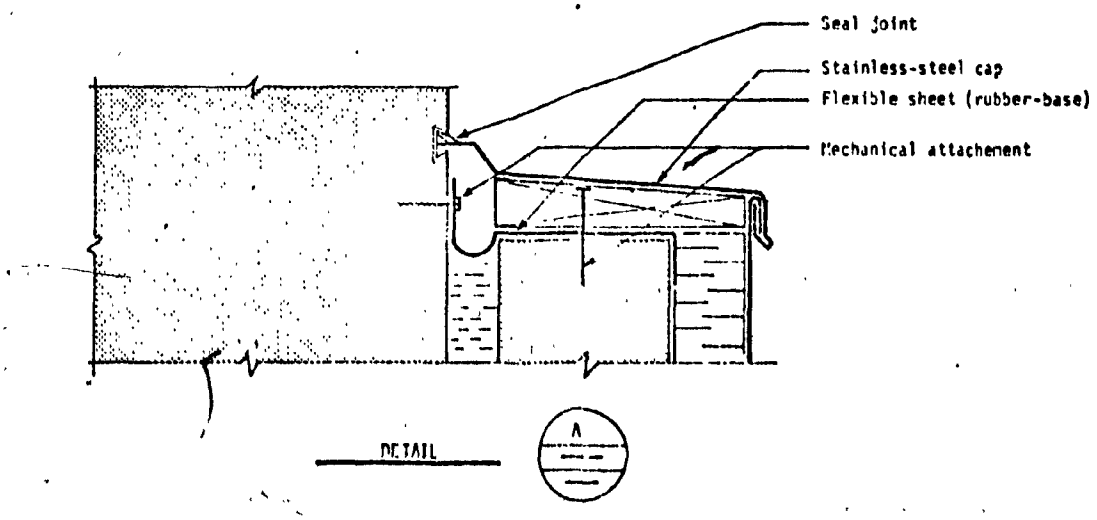

Fig. 3.1 As built typical cross section for the powerhouse roof.

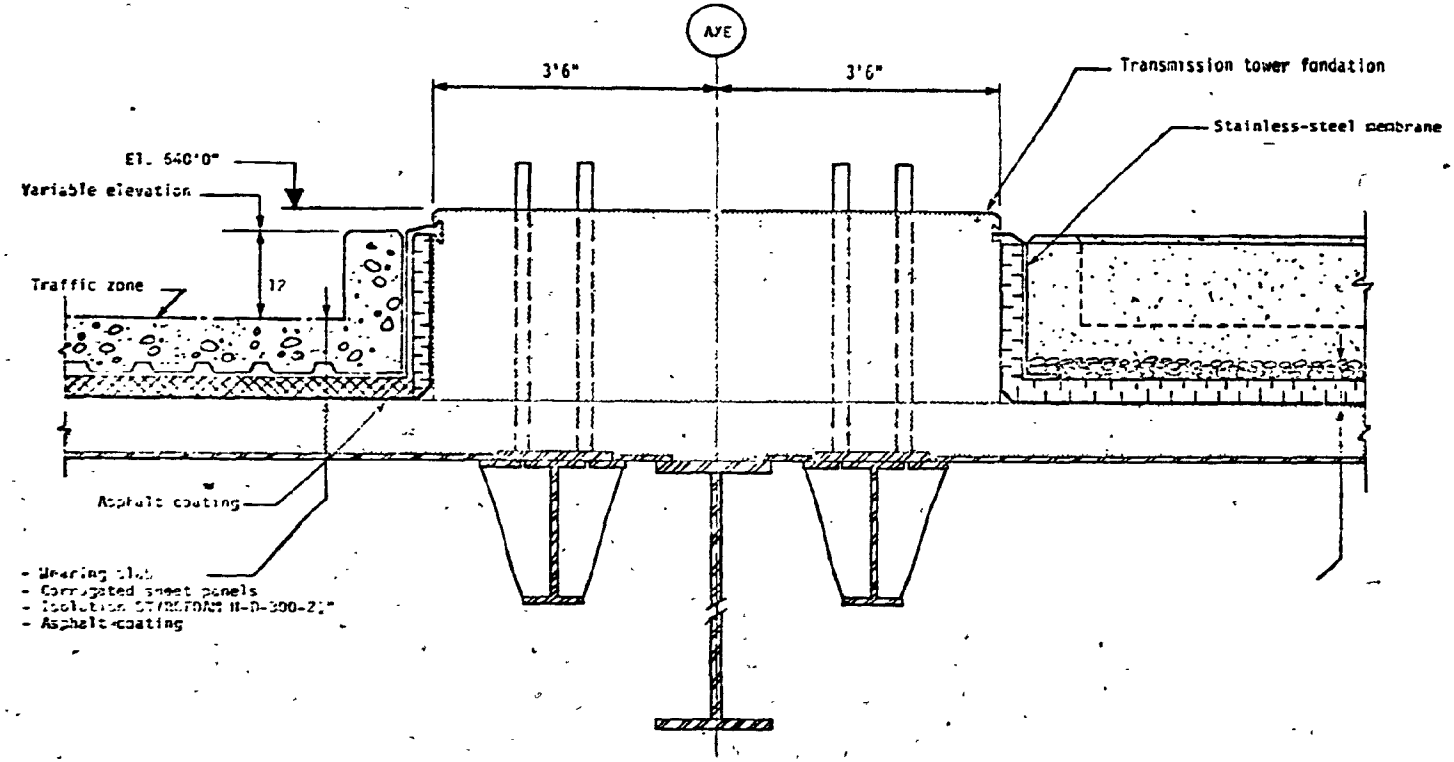

Fig. 3.2 Details of the transmission tower base on top of the roof.

Special arrangements had to be made on certain sections of the roof, where electrical installations would create complicated load conditions. Such is the case for the series of beams which support the nine 500 ton transformers and the 35 foot high fire walls which seperate them. Special attachements had to be designed underneath the transmission line towers in order to transfer the external forces of each tower to the adjacent main girder. For the main steel columns that support the roof and crane beam, two alternatives were studied:

1- Seperate columns (crane beam columns not tied to the building columns).

2- Single columns (the two columns replaced by one stepped column).

The result of these studies favored the stepped columns which were more economical, more aesthetic and easier to errect, as shown on Fig. 3.3.

3.1 Technical Specifications

The technical specifications required that all material used for the fabrication of permanent element be new, and that the contractor produce a mill test certificate for all steel used. Fabrication had to be carried out in accordance with the CSA standard specifications S16-1969.

These specification also indicated that the steel panel roof

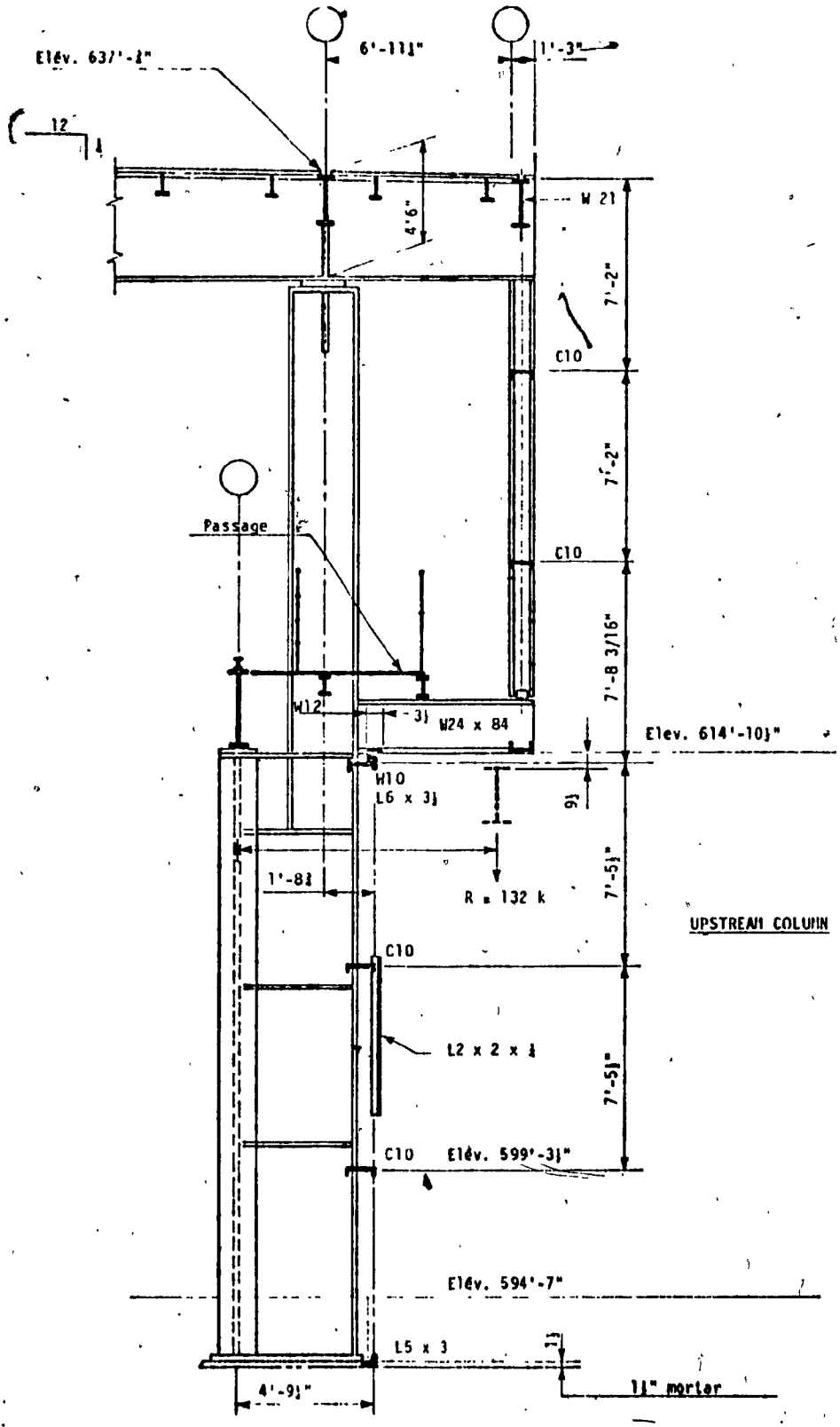

Fig. 3.3 Stepped column detail.

should be fabricated in such a way as to obtain a perfectly water-tight seal. Each panel plate must be in one piece, if not all assembly welds should be shop tested for water-tightness using an approved method. All necessary precautions were taken during the fabrication and the welding of the steel roof panels in order to respect the following tolerances.

a) Squareness:

Out of square shall be less than or equal to:

$(\frac{1}{16} \times \frac{L}{10})$ in inches

where L = Length or width of panel in feet.

b) Deviation from flatness

D = width of panel in inches

t = thickness of plate in inches

d = Least distance between stiffeners in inches

For $\frac{D}{t} > 100$, the maximum deviation between two stiffeners: must be less than or equal to $\frac{d}{67}$ in inches; and $\frac{d}{34}$ between a stiffener and the edge of a panel.

3.2 Delivery and erection

As previously mentioned, all of the steel elements of the

superstructure, including the roof panels, were fabricated in accordance to the Canadian Steel Code S16. In general no real problem was encountered in transporting the heavy pieces such as the columns, girders, etc. However, for the roof panels, in spite of the fact that stiffeners were added to increase their rigidity, their ¼ inch thickness proved to be insufficient for the long trip to the site. On their arrival, the roof panels were visually examined. For the first two roof sections, consisting of 320 panels, major repairs were required. Most of these repairs were carried out either in the storage yard or on the roof during panel installation. In general repairs were needed to bring the panel's edges to the allowable tolerances mentioned in section 3.1 and to allow the welding of each panel to an adjacent panel or to the supporting beam.

In order to complete the erection of the superstructure, the contractor used three cranes each with a different capacity and function.

- A 165 ton crawler crane was positioned downstream of the structure to lift and install the columns and longer sections of the main girder.
- A 50 ton mobile crane was used for general steel handling.
- A 60 ton mobile crane was positioned upstream of the structure on the service road at the same elevation as the roof. This crane was used to complete the erection by placing elements that could not be reached by the 165 ton crawler crane.

From the beginning of erection, standard procedures of control were adopted and final checking was carried out when the part of the

structure between two contraction/expansion joints was completed. However, due to the unusually high quantity of welding required, the vulnerability of the structure to displace caused a serious problem of alignment at the contraction joints. Roof panels had to be removed and rewelded between lines # 13 to # 16 in order to respect the required clearance at the contraction joint. Following such difficulties, a thourough examination of the structure's behaviour was conducted in order to establish a control plan that would prevent similar problems with the remaining sections.

The main points of this plan are listed below:

1- Beams, columns, girders

The Owner's approval was required at the completion of each phase of erection mentioned here below. No further work was allowed before all errors in the previous phase of erection had been corrected.

a) The top elevation of the base plate was verified and shimmed wherever necessary.

b) The anchor bolts were positioned inside the sleeves within the allowable tolerance of ± 1/16 of an inch at the four holes of the bottom flange of the columns. The bolts were then checked in the North South and East West direction where the maximum deviation of ± 1/8 of an inch was allowed, Fig. 3.4 and 3.5.

c) Columns were placed and an initial torque was applied

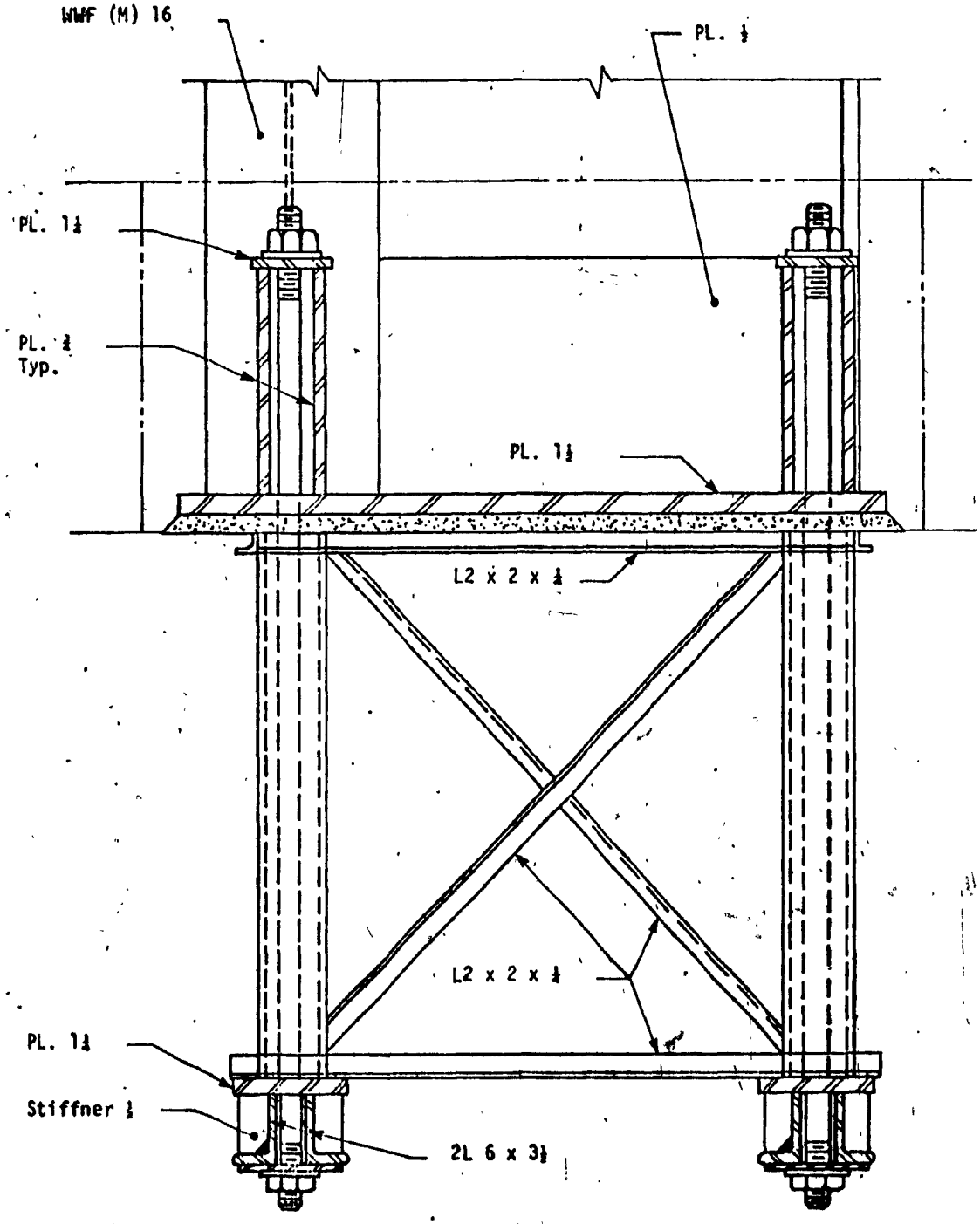

Fig. 3.4 TYPICAL DETAIL FOR MAIN COLUMNS AT FOUNDATION LEVEL - E-W VIEW

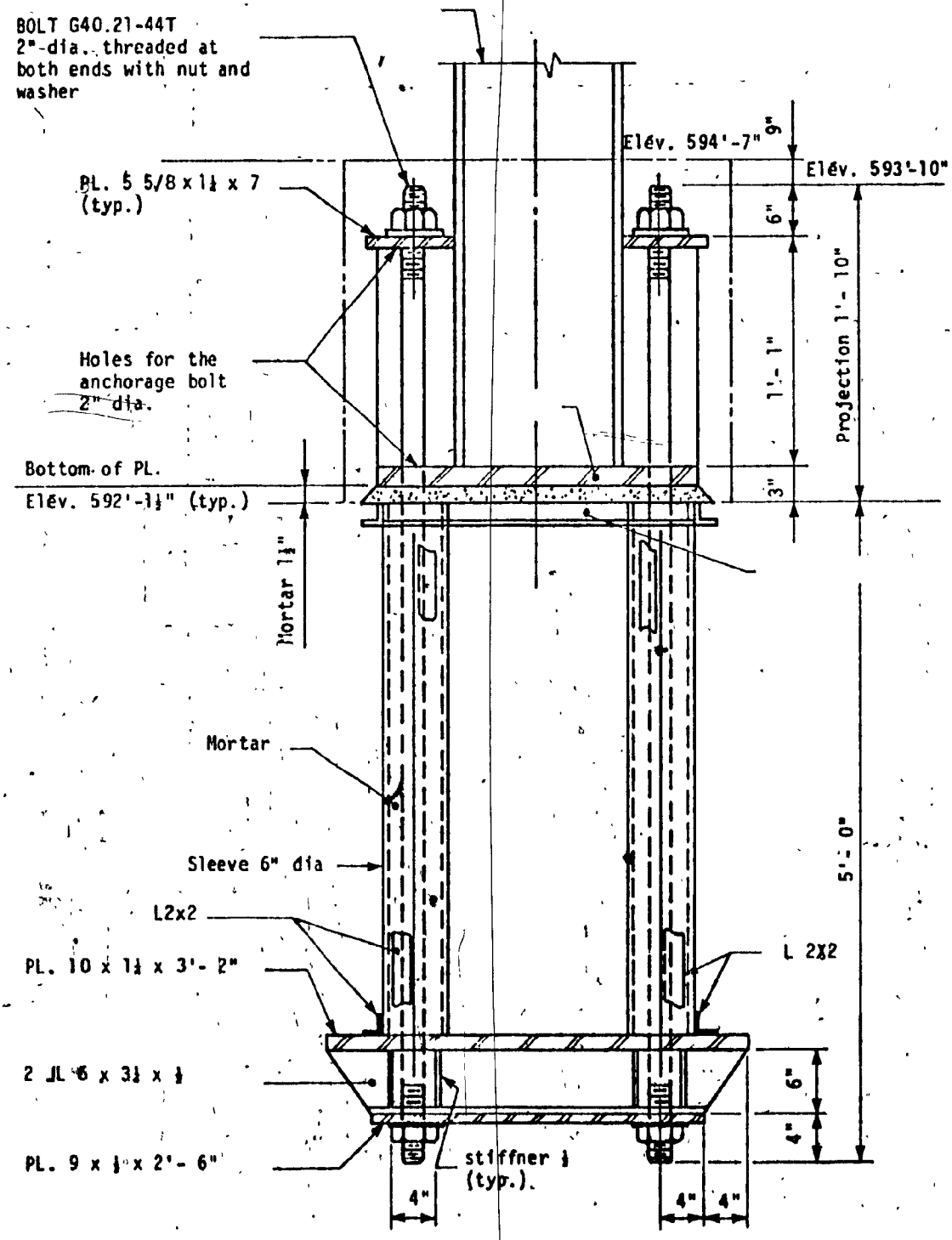

Fig. 3.5 TYPICAL DETAIL FOR MAIN COLUMNS AT FOUNDATION LEVEL - N-S VIEW

to the bolts. Then, erection proceeded to the main girder and remaining beams with an initial torque as applied to the connected bolts.

d) The columns were plumbed in the North-South and East-West directions.

e) The final torque on all the connecting bolts was applied if the section located between two contraction-expansion joints was within tolerance otherwise, steps (a) to (e) were repeated until the final adjustment was complete. During erection, special attention was given to the bridge beam and its theoretical elevation was checked at the intersection of each column.

2- Placing of the roof panels:

a) Roof panels were separately identified according to the numbering system specified on the drawings. Each panel was placed in its correct position, and fixed to the top flange of the supporting beam by two spot welds.

b) The same procedure was repeated until the whole roof section between two contraction/expansion joints was completely covered.

c) All required repairs or corrections were done at the border lines between the panels and at the joint between the panels and the roof beams.

3,3 Welding the roof panels

On site three types of welding were performed on the roof components:

a) Fillet welds were applied between the WT'9 of the roof panels and the webs of the main girders, and also between the flanges of the main girders and the edges of the panels.

b) Square groove welds were performed between each panel.

c) Sl[illegible] welds were carried out at the top flanges of each part of the main beam.

Welding the roof panels (Fig 3.6, 3.7 and 3.8) was a long and complicated task, and many different problems arose during this activity. First, due to the sensitivity of the panels to any change in ambient temperature, the gap between the panels had to be checked and adjusted continuously at the contraction joints. This sensitivity to temperature change had further implications on determining the part of the roof that had to be adjusted and welded before the end of each working shift. Secondly, the movement of the structure caused by the heat generated during the welding process was another significant factor, specially when welding was performed following no specific pattern. The first problem was solved by insuring that individual sections of the roof were completed during one shift. In order to solve the second problem the procedure mentioned hereafter was employed, and as a result the structure's movement during erection was reduced and controlled.

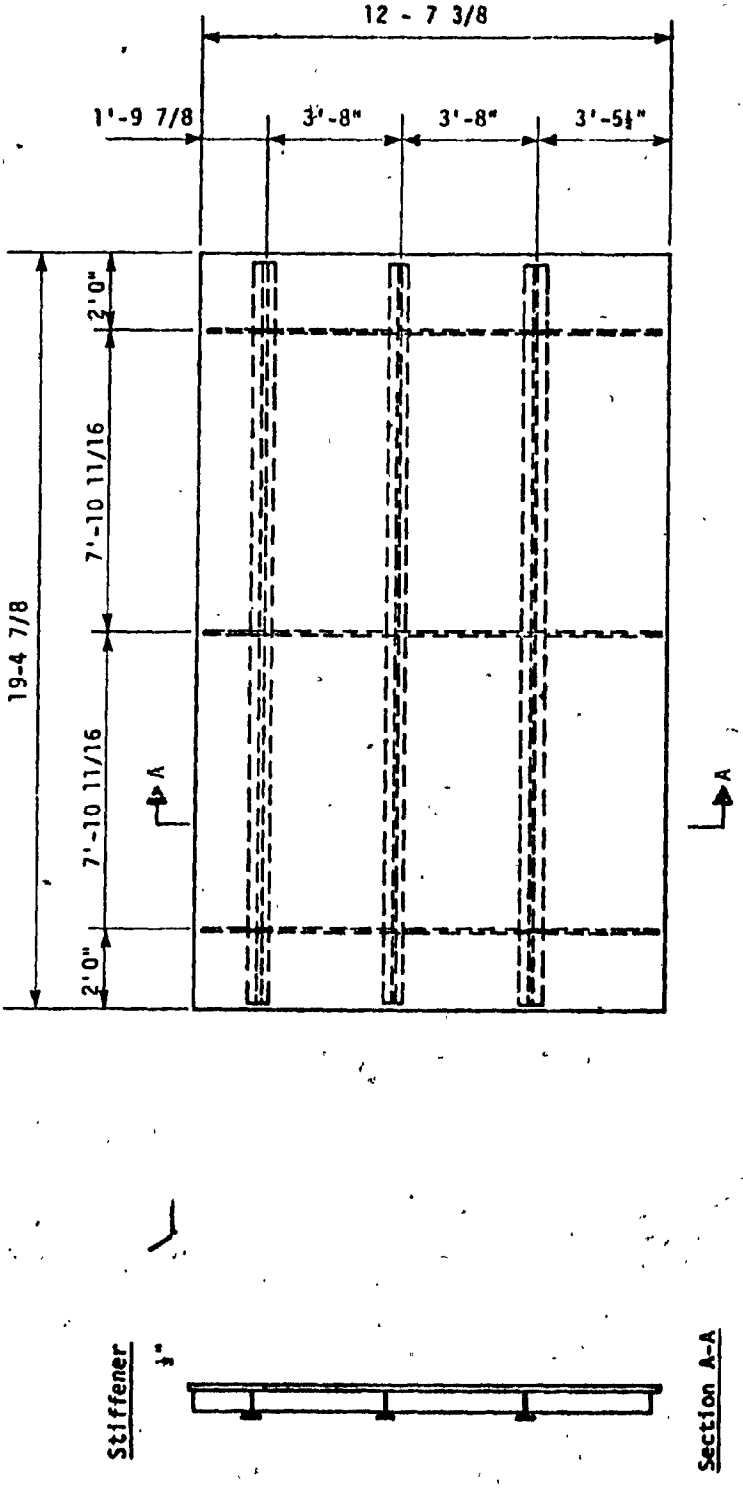

Fig. 3.6 Typical roof Panel.

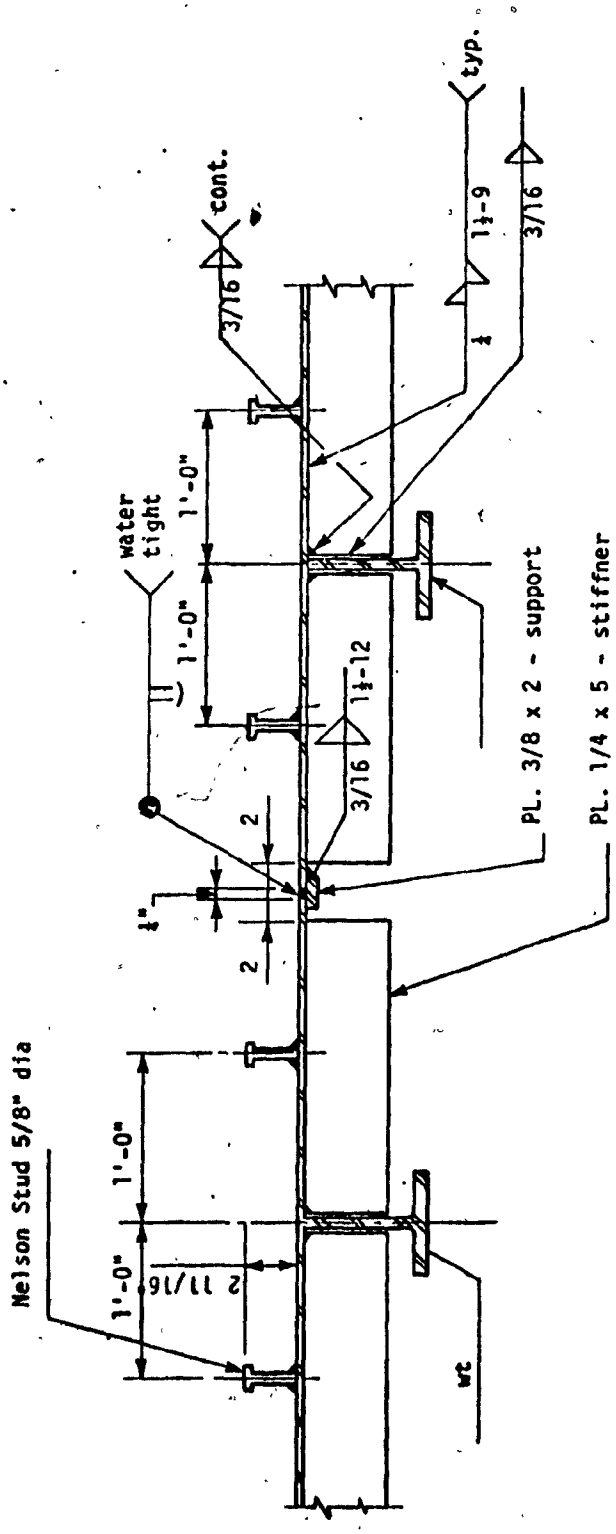

Fig. 3.7 TYPICAL CONNECTION BETHEEN TWO PANELS

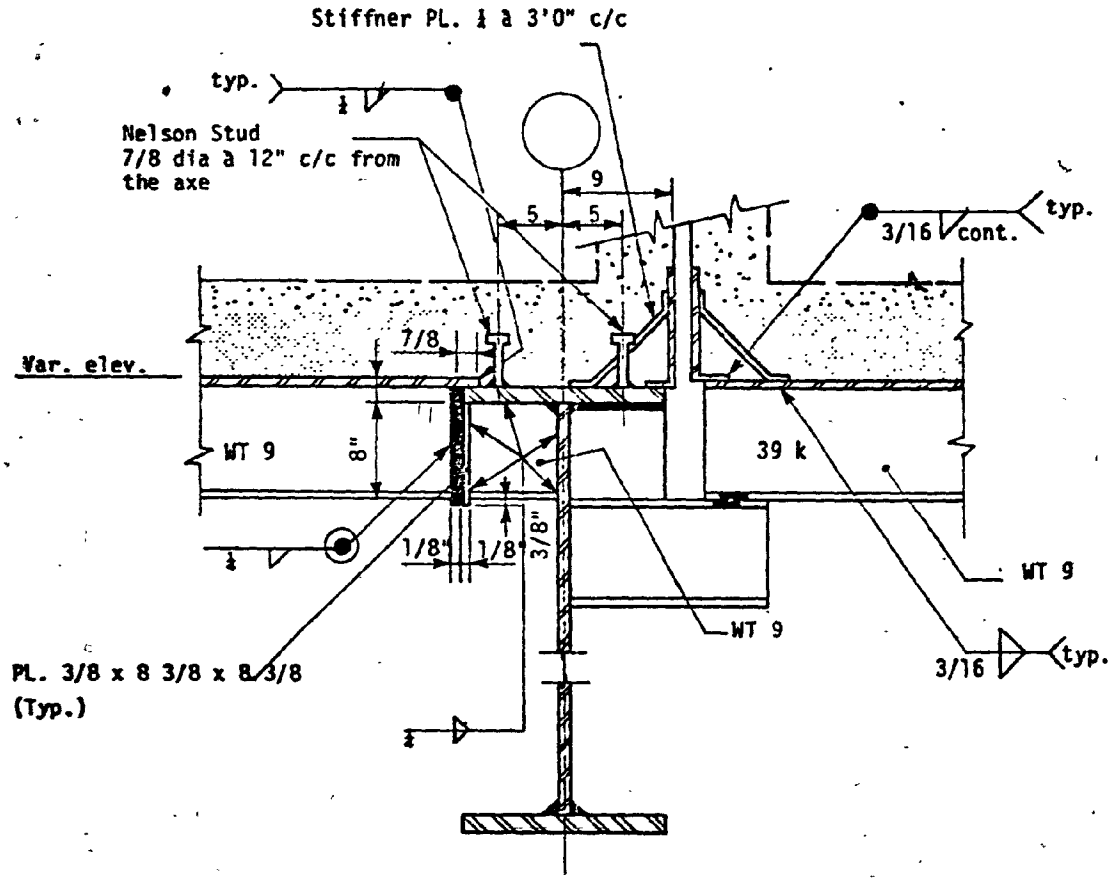

Fig. 3.8 TYPICAL CONNECTION AT CONTRACTION/EXPANSION JOINT

3.4 Welding Procedure (see Fig. 3.9, on page 64 for typical section)

3.4.1 Connecting the WT9's to the main girders

a) All panels were tack welded along their edges for 2 inches every 12 inches in both longitudinal and transversal directions.

b) Structural welding began with panels located midway between the contraction-expansion joints (ie. line 25).

c) Both sides of the web of the central WT9 of each panel were welded to the main girder as shown in Fig. 3.9. This procedure was adapted on subsequent panels along the same line.

d) The remaining WT9's of each panel (two in general) were then welded to the main girder, always along the same line (ie. line 25).

e) The flanges of each WT9 were welded in a similar manner, thus completing all structural welds on this first line (line 25).

f) Steps c, d, and e, were then repeated on adjacent lines (ie lines 24 and 26) simultaneously.

g) Welding then progressed outwardly in a similar fashion.

3.4.2 Joining the panels together

The joints between panels were welded in two passes (see

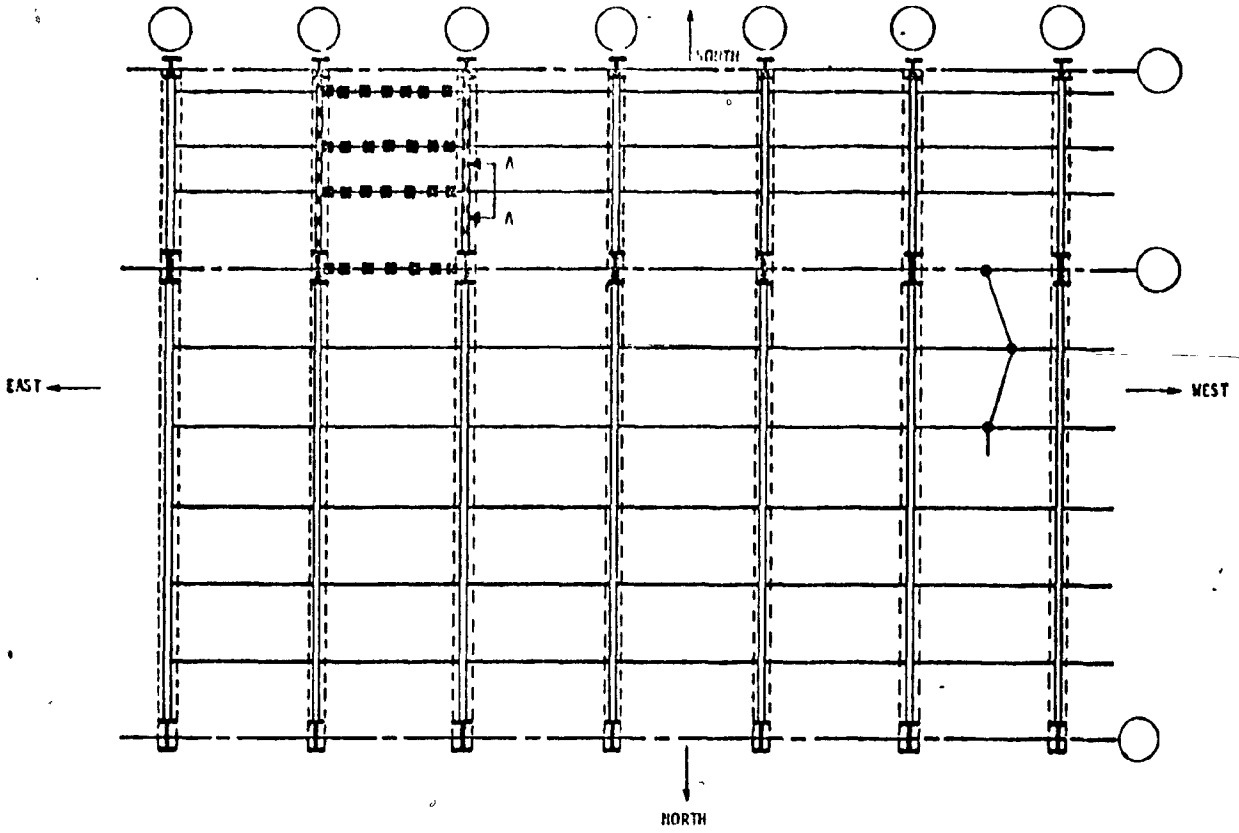

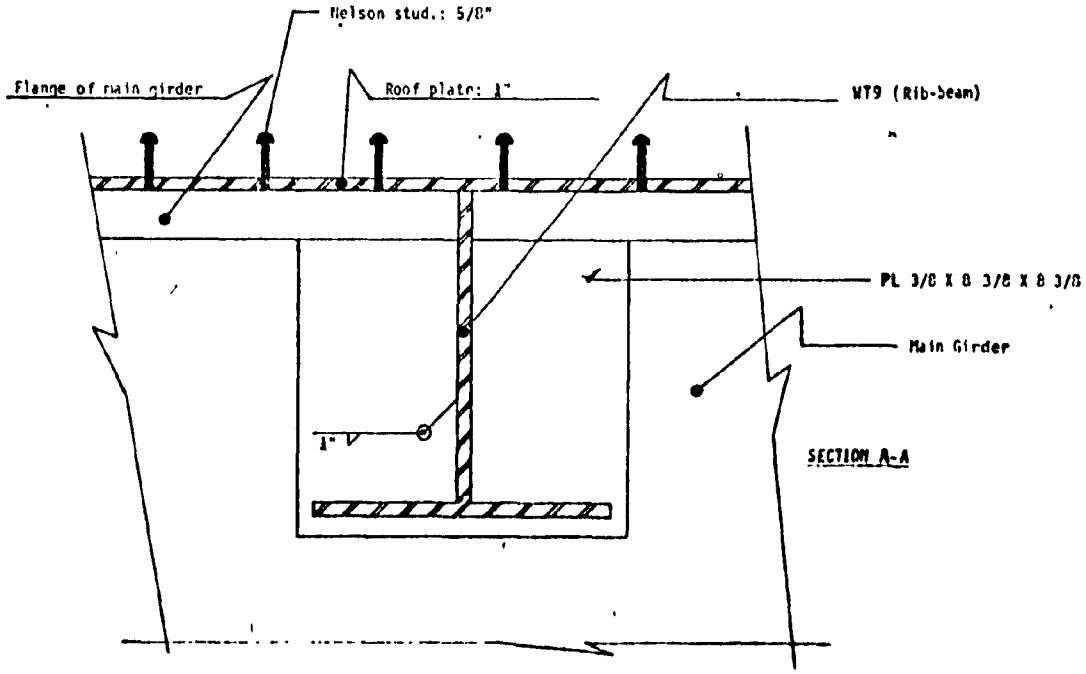

Fig. 3.9 Welding the rib-beam with the main girder.

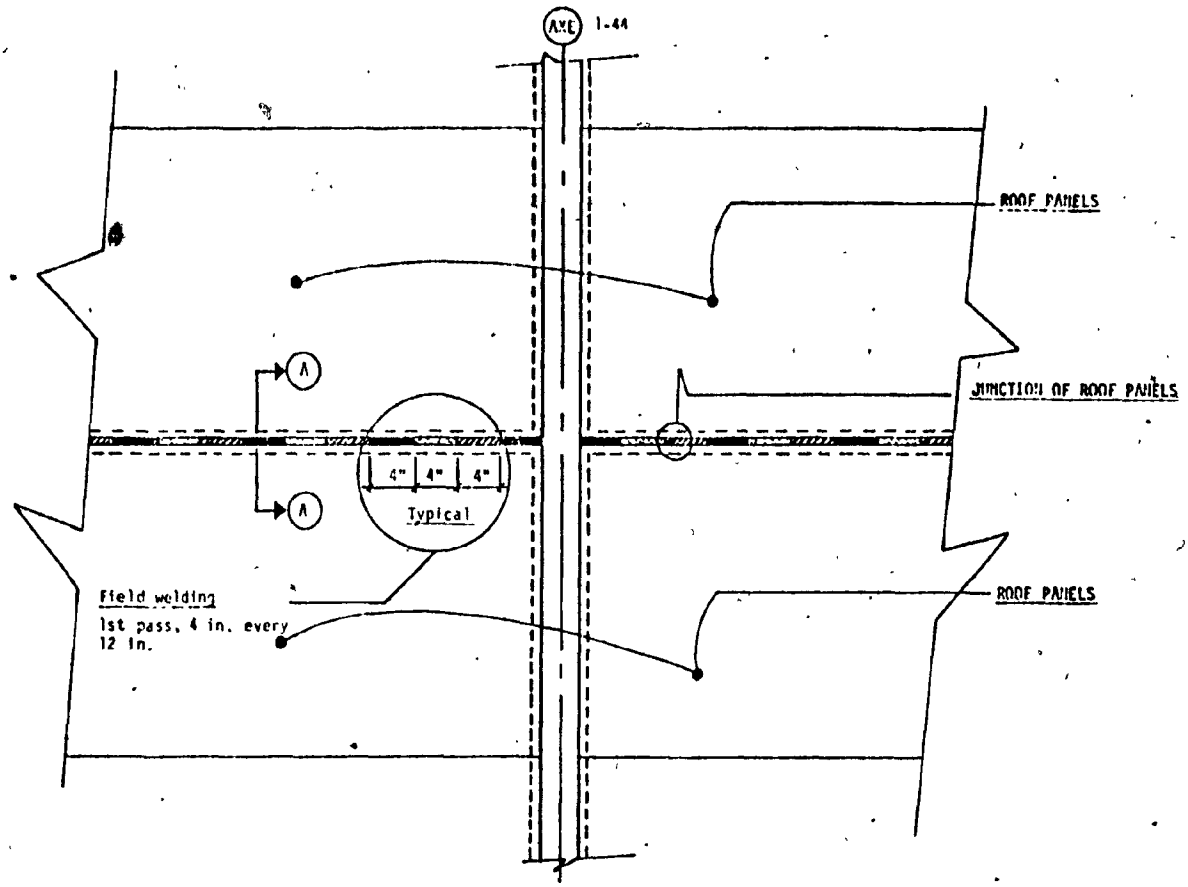

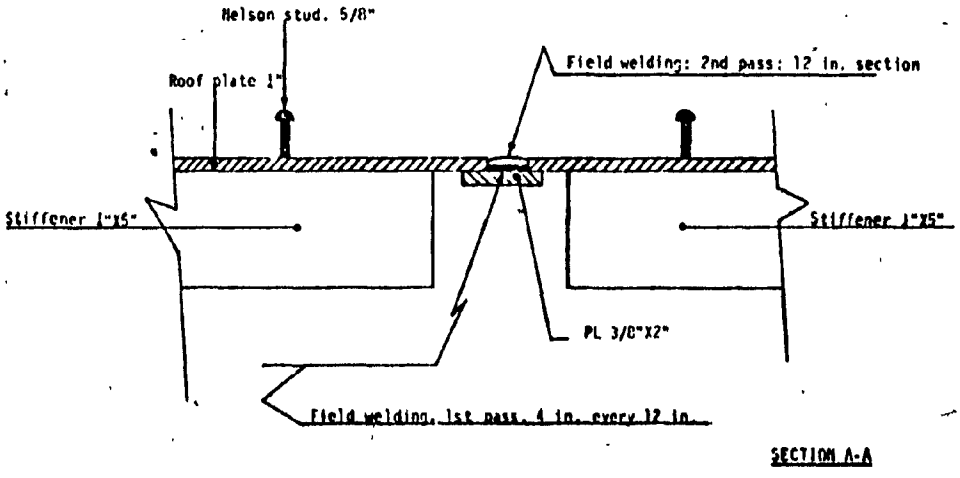

Fig. 3.10 Welding two panels together.

Fig. 3.10). The first pass actually consisted of three passes, as weld was applied for 4 inches every 12 inches. The second, was performed in two passes of 12 inches every 24 inches. (see Fig. 3.10).

3.5 Examination of welds

Visual inspection was required for all welds as indicated in the CSA standard, however the steel erector is obliged contractually to perform several (a total of four) types of non-destructive tests. These tests, with their extent of application are listed below:

Member	Examination	Extent
Beams WT9 (fillet welds)	Magnetic particle	100%
Main beams (slot welds on the top flanges)	X-Ray	100%
Contact lines between all roof panels, and between the panels and the upper flanges of the main beams	Magnetic particle	25%
Water tightness of roof panels	Vacuum testing	100%

A typical liquid penetrant examination procedure is also performed on all the rods that were welded to the roof for anchoring the transmission line tower concrete bases to the roof.

A brief resume of these procedures is outlined in the following paragraphs.

3.5.1 Vacuum Testing

The Vacuum Test is conveniently performed by means of a metal testing box 6 inches wide by 30 inches long, with a glass window in the top. The open bottom is sealed against the steel plate surface where the two panels are connected together by a sponge rubber gasket.

Approximately 30 inches of the seam under examination is brushed with a soapsuds solution or linseed oil. In freezing weather a nonfreezong solution may be necessary. The vacuum box is placed under the coated section of the seam and a vacuum is applied to the box. The presence of porosity in the seam is indicated by bubbles or foam produced by air sucked through the welded seam.

A vacuum is created in the box by any convenient method, such as connection to a gasoline or diesel motor intake manifold or to an air ejector or a special vacuum pump. The gauge can register change of vacuum of 2 psi or more.

3.5.2 Magnetic Particle Examination Procedure

This procedure describes the basic procedure to be followed for magnetic particle examination of a weld using the dry powder method, and provides for local circular magnetization by the use of prod type contacts, or an A.C.Yoke. (see photo no. 6). Magnetization is

applied via portable prod contacts connected to the unit by either flexible cables or an A.C.Yoke. A remote control switch, built into the prod or yoke handle, permits the technician to turn the current on, after the prods or poles have been properly positioned on the part being examined, and to turn the current off before they are removed.

Prior to the application of the powder, the surface to be examined was cleaned and freed of dirt, grease, oil or any other extraneous material that would interfere with the examination. The red powder provided adequate contrast with the background of the surface being examined.

At least two separate examinations were conveyed on each area. The welds were examined with the poles placed in such a manner that the lines of flux in the first examination were approximately perpendicular to the lines of flux of the second examination. All dubious indications were considered unacceptable, and the area had to be repaired until further examination showed no possible deficiency.

3.5.3 Liquid Penetrant Examination procedure

This non-destructive test may be considered as an extension of the visual inspection. To carry-out this test, the surface to be examined should be dry and free of dirt. The pre-cleaning was carried out using a methyl hydrate solvent and lint free rags. After pre-cleaning, the surface was thoroughly dried to ensure that no solvent remains to hinder the capillary action of the penetrant. A minimum of five (5) minutes was allowed to permit complete evaporation of the methyl

hydrate before applying the penetrant to the surface under examination.

The penetrant was applied by either brushing or spraying. The penetration time shall be a minimum of ten (10) minutes duration and the material surface temperature should be between 60^{o} F and 125^{o} F. No removal of excess penetrant was allowed before the required penetration time had elapsed. The developer was then applied sparingly in a thin even coat. Final examination was made after allowing the penetrant to bleed off for a period of between 7 and 30 minutes. Mechanical discontinuities at the surface were indicated by the bleeding penetrant. All defects were marked directly on the surface. Necessary repairs were carried out in accordance with specifications, and the areas were re-examined.

It should be noted that the advantages of this test (rapidity and low cost) are limited by the fact that only surface defects can be located. All defects that are determined using this method are merely indicative and no quantitative results concerning the depth or gravity of the defect can be obtained.

Finally, in order to complete the assembly of the roof panels, a total of 9469 man-hours was required in order to weld a total of 13.3 miles, using 110 miles of welding rods. The actual cost of the roof is 62.14 $ per square foot.

PHOTO NO. 1: LG-3 Powerhouse Steel Structure.

Downstream Section of the LG-3 powerhouse superstructure. Note the part of the main girder which is supported by the concrete base and the steel columns. Also, shown is the bridge crane beam above the mezzanine level supported by the main step-columns every 23'-8".

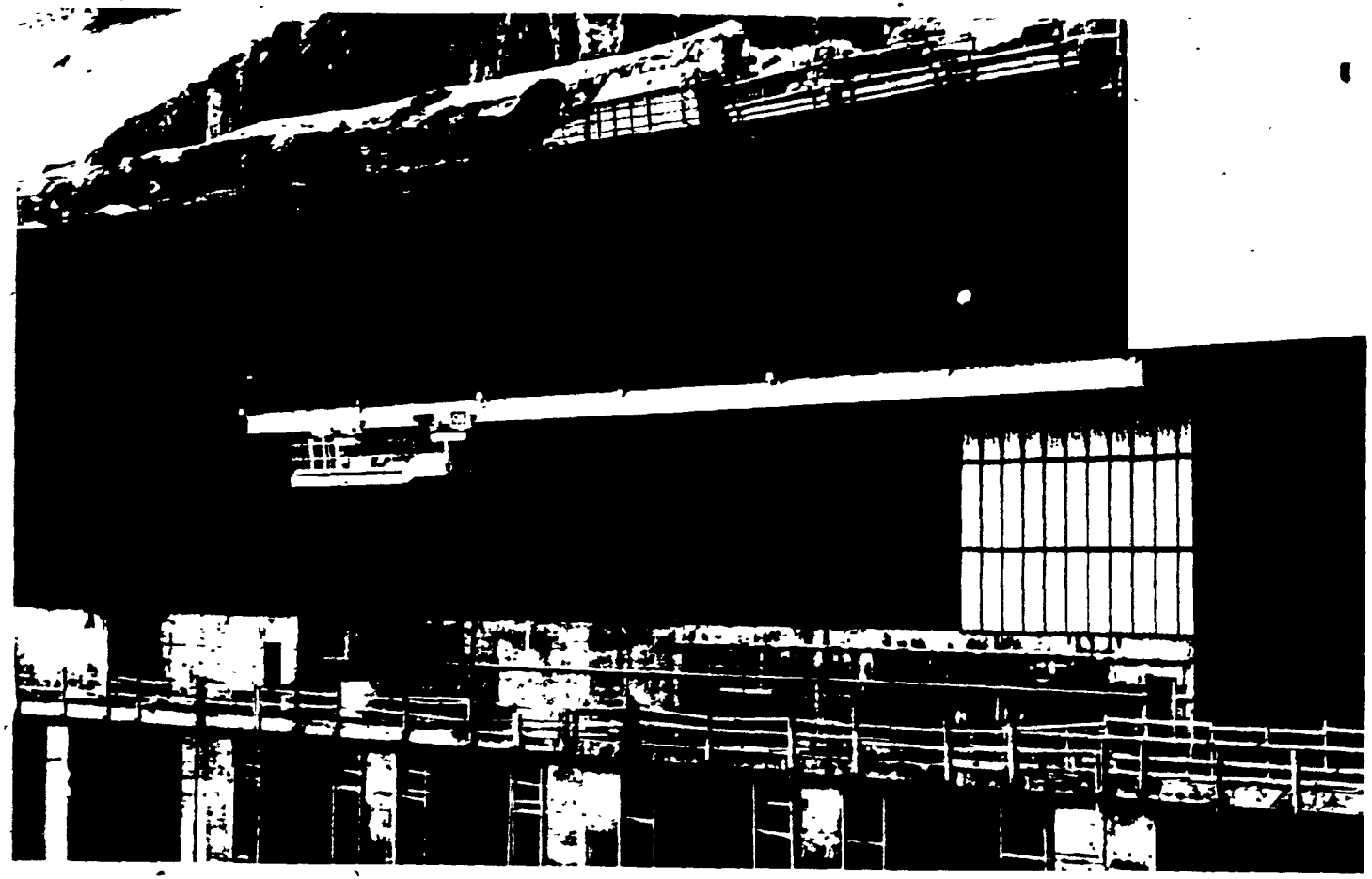

PHOTO NO. 2: LG-3 Powerhouse during construction.

Outside view of the powerhouse superstructure elements before the completion of the metal cladding. The monorail shown here is for the operation of the draft-tube gates.

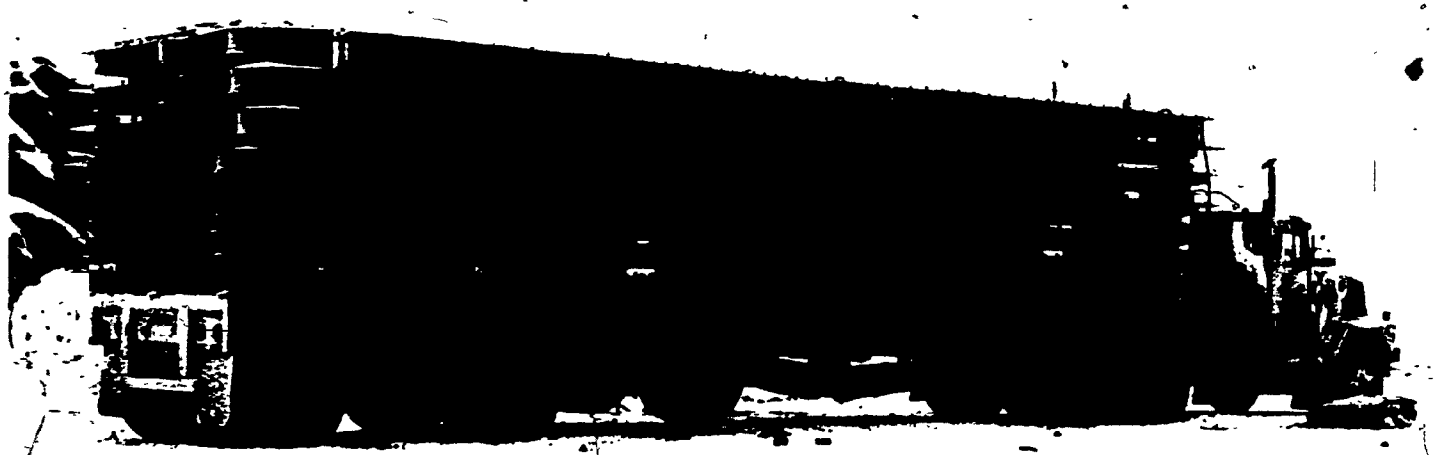

PHOTO NO. 3: Transportation of roof panels.

Delivery of the roof panels to LG-3 site on the spring of 1980. Due to the long road trip, certain damages had occured to the panels and hence, reparations were required.

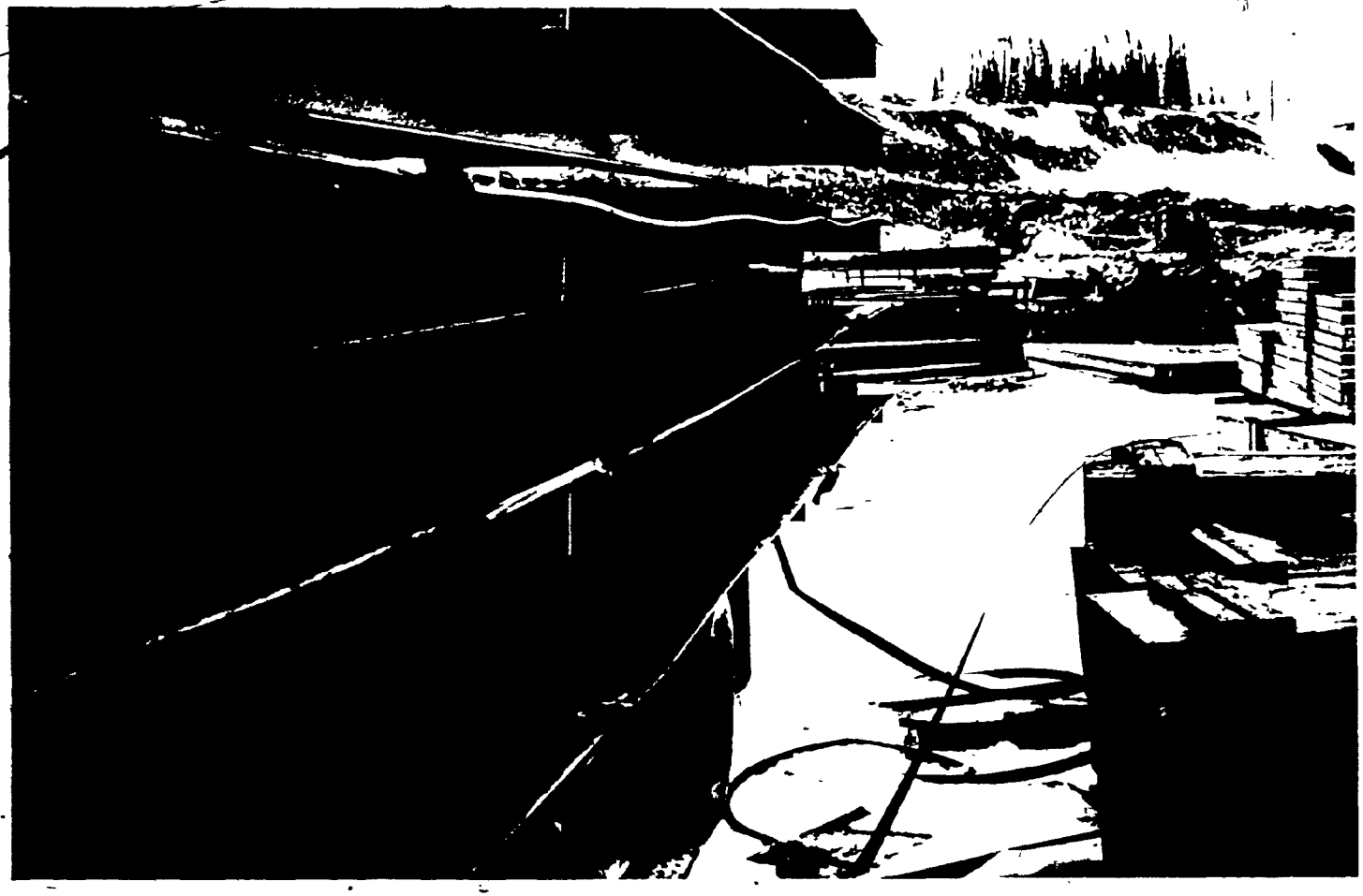

PHOTO NO. 4: Damage to the roof panels.

Warping and surface damages were the main two defects that occured during the transportation of the panels. Notice the stiffeners which were added to each panel to reinforce them during the transportation and erection. Also note that the shear connectors were shop welded, thus reducing field costs.

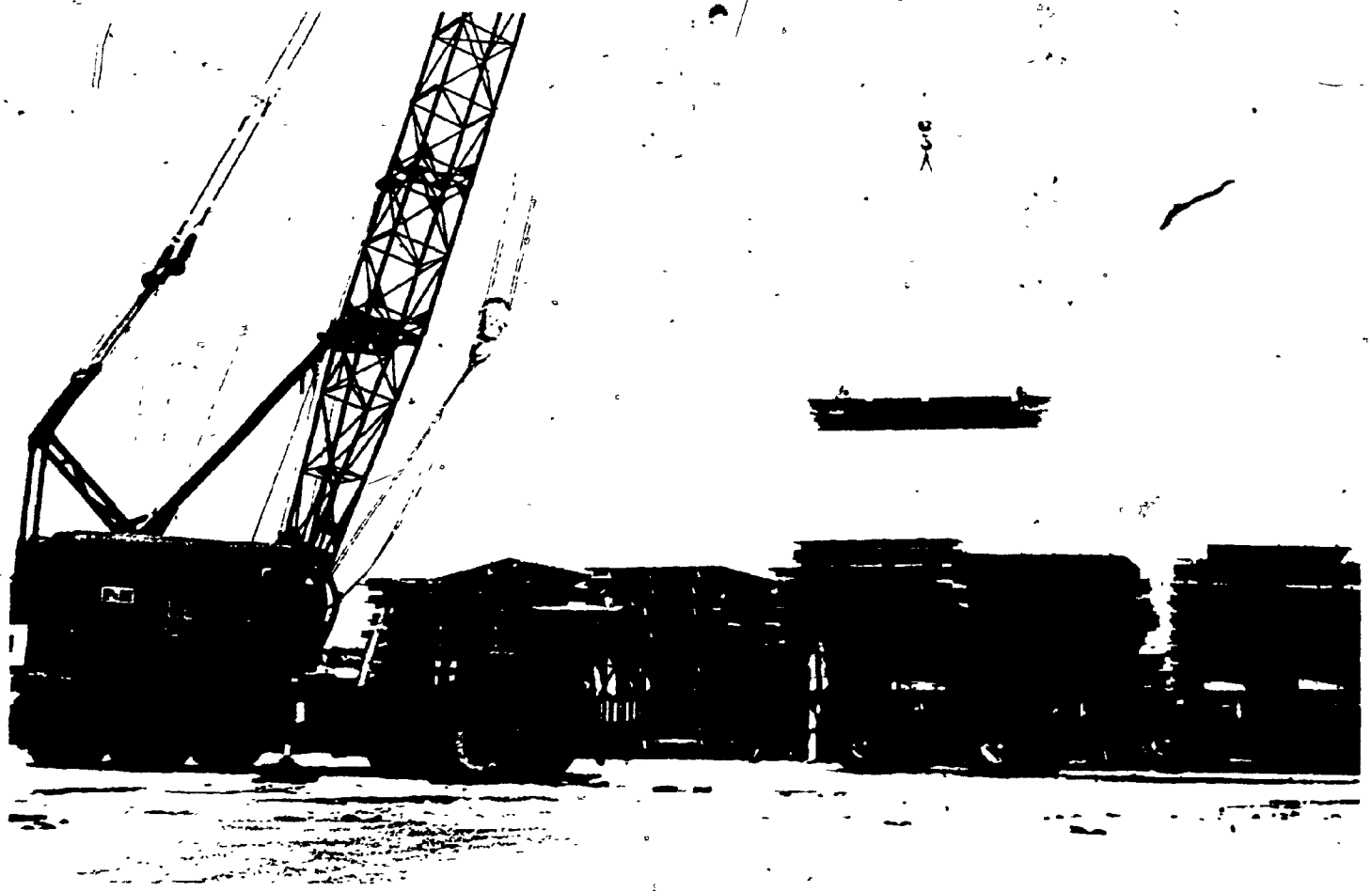

PHOTO NO. 5: Unloading of roof panels.

Unloading the roof panel, was carried out following a spedific pattern. The panels were piled according to the order in which they would be erected.

PHOTO NO. 6: Examination of welds.

The examination of welds using the magnetic particle procedure is shown.

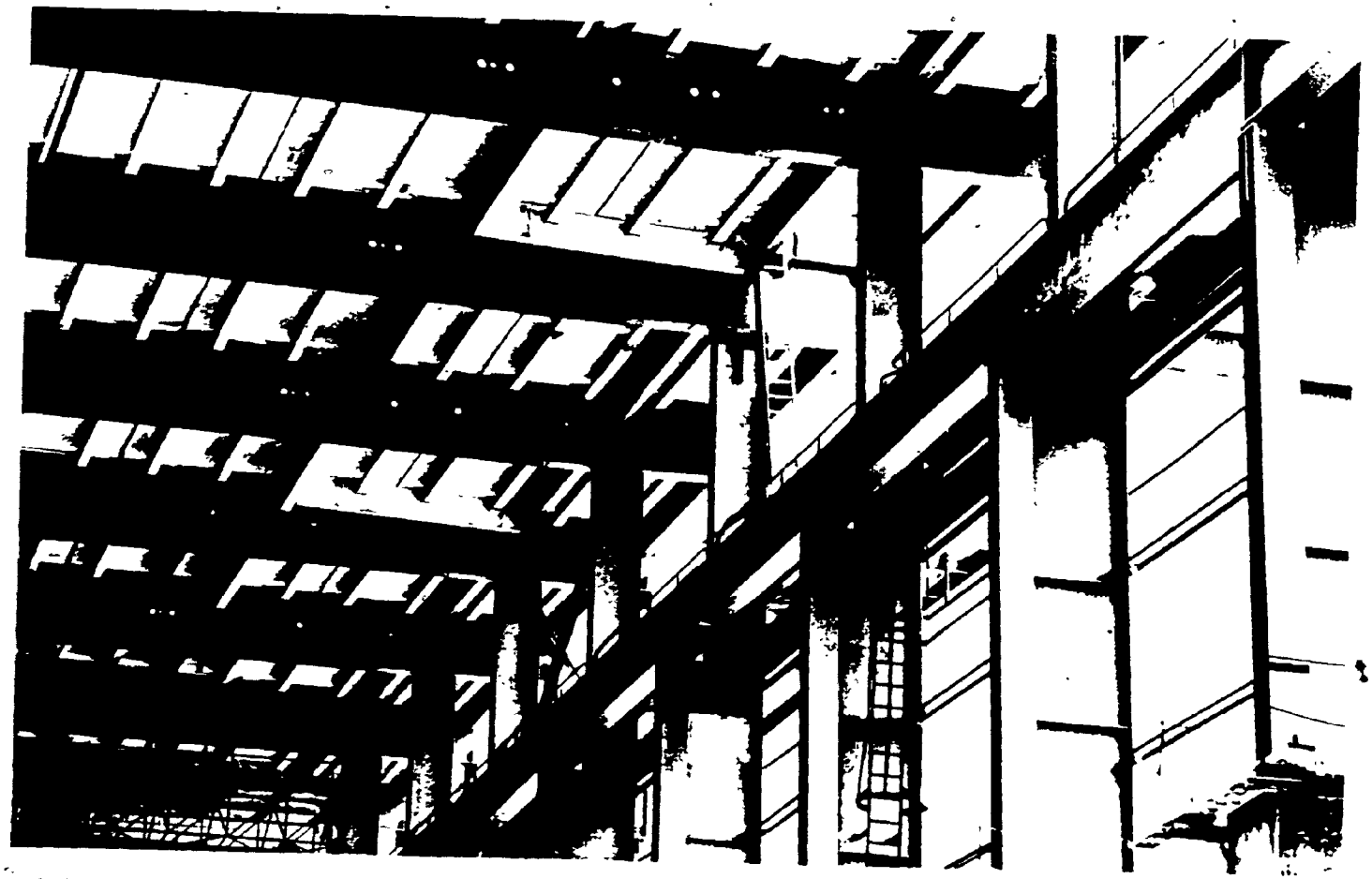

PHOTO NO. 7: LG-3 Powerhouse - Steel-Structure.

View of the Upstream section of the Powerhouse superstructure. Note the mobile platform that is shown at the bottom left of the photo. The contractor used this platform to complete all overhead welding of the webs and flanges of the WT9's on each panel.

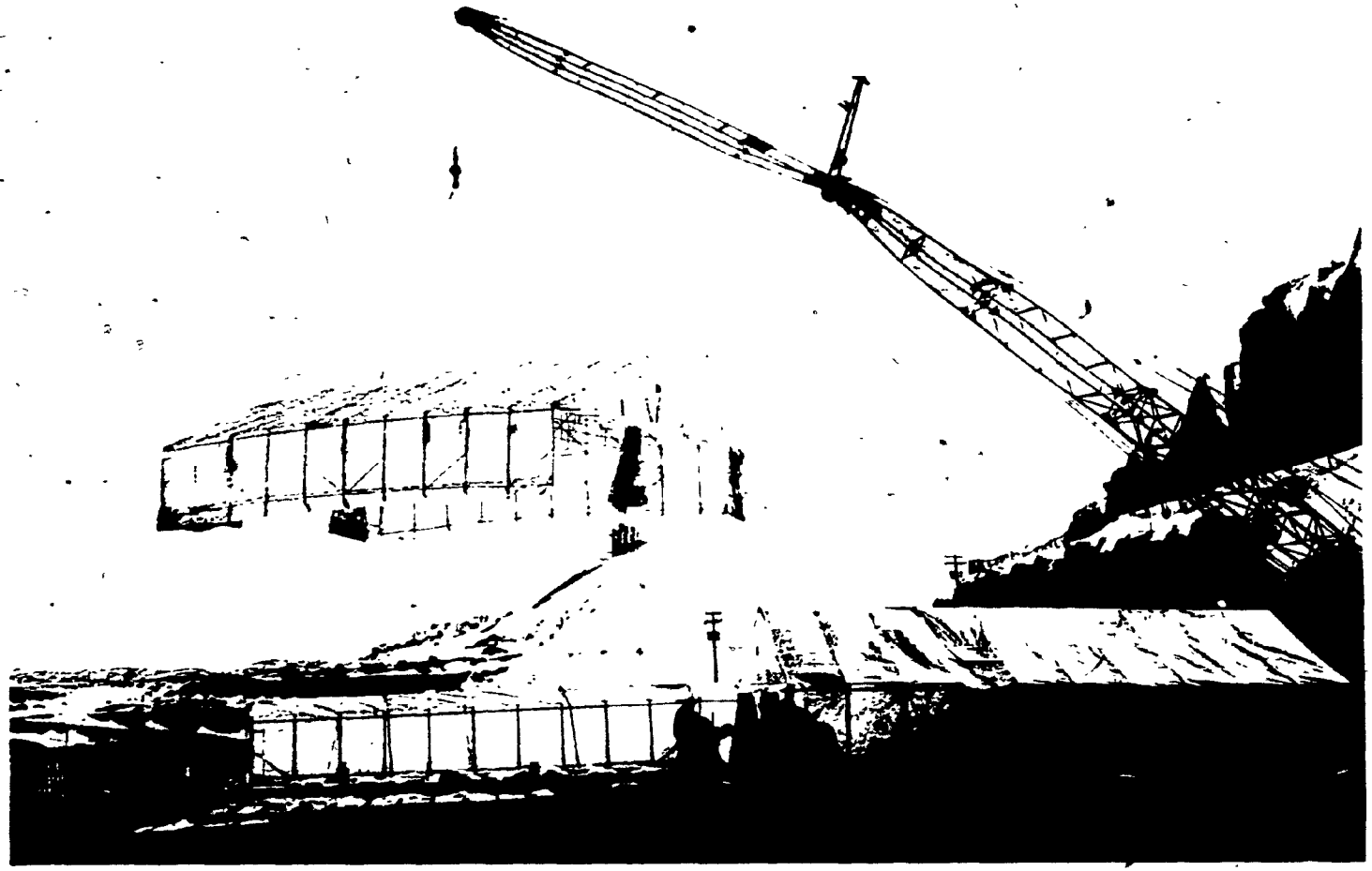

PHOTO NO. 8: Welding during winter months.

In order to respect the minimum temperature requirements of the technical specifications, the contractor had to build light-weight aluminum shelters (30' x 40' and 12' x 40'). Those shelters were heated durint the winter months. All welds were conducted in an ambient temperature of between 5 - 10°c. Those shelters were also useful during rainy and windy periods.

PHOTO NO. 9: Welding of roof panels.

Continuous welding of the roof panels was avoided due to the considerable amount of heat dissipation which caused serious problems in joining a few panels of the roof. As a result welds between the panels and main girders were carried out in steps as shown here.

PHOTO NO. 10: Winter protection of roof panels.

An inside view ofthe shelder where welding proceeds under warm and agreeable conditions in spite of the severe climate outside.

PHOTO NO. 11: LG-3 powerhouse general view during construction.

An East-West look at the powerhouse during construction on March 1981. Note the sides of the mobile platform which were built to form a closed shelter. Heat was also applied to the panels from below.

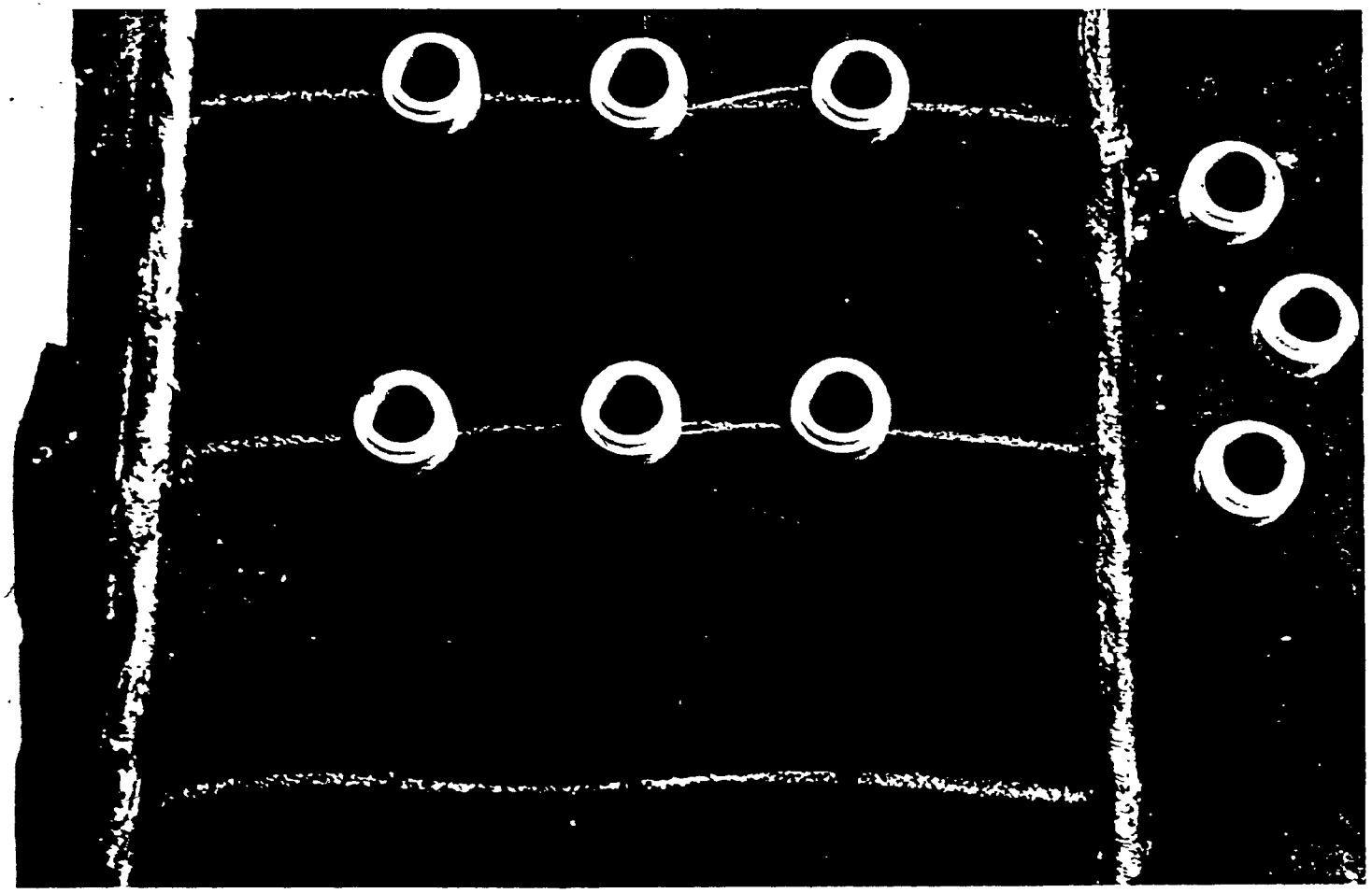

PHOTO NO. 12: Welding of Nelson shear-studs.

Prior to welding, ceramic ferrules were places on top flange of the main-girder and the shear connectors were inserted.

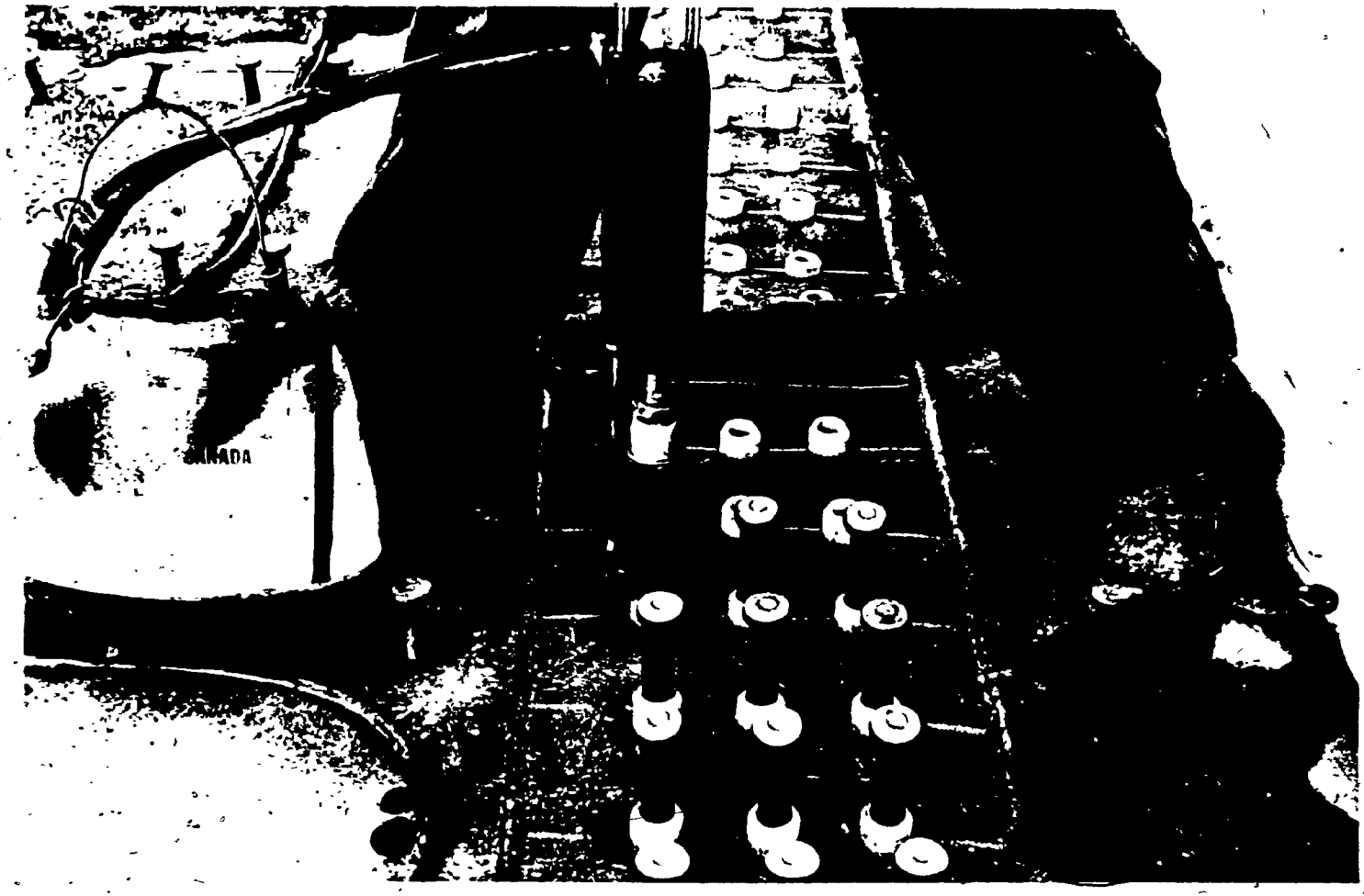

PHOTO NO. 13: Welding of Nelson Shear-Stud.

A special welding gun was used to connect the studs to the steel surface.

PHOTO NO. 14: LG-3 powerhouse steel structure.

A West-East view of the powerhouse during construction showing the mobile welding platform.

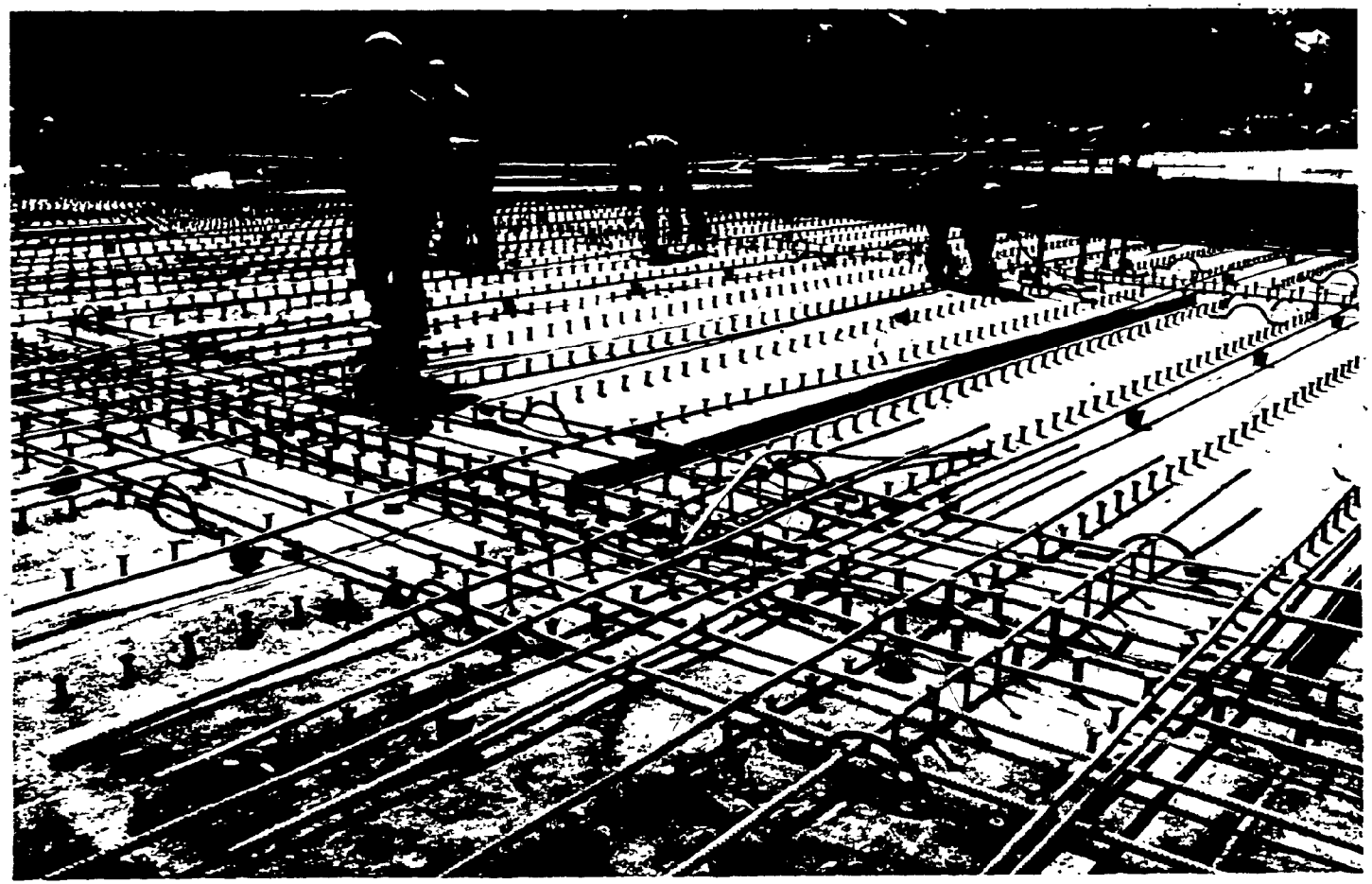

PHOTO NO. 15: Placing reinforcement bars on the roof.

Upon completion of the roof panels welds, the surface was cleaned and washed and reinforcement bars were placed.

PHOTO NO. 16: Concreting of the roof.

Concreting of the structural slab was carried out between each expansion/contraction joint (96 - 120 feet) using a concrete pump. Adjusting the slopes and finishing the surface was a difficult job requiring a great deal skill.

BIBLIOGRAPHY

1. M.S. Triotsky, "Orthotropic Bridges Theory and Design", The James F. Lincoln Are Welding Foundation - Cleveland Ohio August 1967.

2. American Institute of Steel Construction, "Orthotropic Steel Plate Deck Bridges" 1963.

3. Canadian Institute of Steel Construction, "Handbook Of Steel Construction" April 1979.

4. Raymond J. Roark and Warren C. Young, "Formulas for Stress and Strain" - McGraw Hill Book Company 1966.

5. K. Ludwig and R. Olive, "James Bay Powerhouses - Layout and Design Criteria", Journal of the Energy Division. ASCE vol. 106, n^{o} EY2, October 1980 pp. 235-255.

6. Hetenyi, M., "Beams on Elastic Foundation", University of Michigan Press 1946.

7. E.J. Yoder, "Principales of Pavement Design" - J. Willey Publisher Inc. New York, fourth printing August 1965 - page 68.